DFPD–99/TH/19
TUM–HEP–333/98

Two-loop heavy top corrections to the Z^0 boson partial widths

Giuseppe Degrassi[a] and Paolo Gambino[b]

[a] *Dipartimento di Fisica, Università di Padova and INFN, Sez. di Padova, via F. Marzolo, 8, I-35131, Padova, Italy.*

[b] *Physik Dept., Technische Universität München, James-Franck-Str., D-85748 Garching, Germany*

Abstract

We present the evaluation of the two-loop $O(g^4 M_t^2/M_W^2)$ effects in the partial widths of the Z^0 boson in the $\overline{\rm MS}$ scheme and in two different implementations of the on-shell scheme. We observe a clear reduction of the scheme dependence of the predictions. The renormalization procedure and the Heavy Top Expansion employed in the $O(g^4 M_t^2/M_W^2)$ calculations are illustrated in some detail and intermediate results are provided. We discuss the implication of our results on the constraints for the Higgs mass making use of simple interpolating formulas. We find that precision data give $M_H < 285$ GeV at 95% C.L. taking into account the theory uncertainty. Including also the information from direct search experiments we obtain a 95% upper bound $M_H < 345$ GeV.

1 Introduction

The impressive amount of data collected at LEP, SLC, and the Tevatron allows for a very stringent test of the Standard Model (SM), at the level of the per mille accuracy. This experimental situation has required a significant effort from the theory side in order to provide predictions for the electroweak observables with comparable precision. We recall that such a level of accuracy tests the quantum structure of the theory, thereby providing information about physics at mass scales that are not directly accessible at our experimental facilities.

After the discovery of the top quark at Tevatron the only mass scale still unknown in the SM is the one related to the Higgs boson. As the sensitivity of the various precision observables to the Higgs mass, M_H, is approximately logarithmic, the extraction of the relevant information is more difficult and delicate than in the case of the top and requires a careful consideration of higher order effects. In the recent past it was recognized [1,2] that in order to obtain accurate constraints on M_H from global fits to the experimental data, the theoretical predictions of the observables most sensitive to M_H should also include two-loop top effects enhanced by factors $(M_t^2/M_W^2)^n\,(n=1,2)$. This observation called for the study of the $O(g^4 M_t^2/M_W^2)$ corrections to the $M_W - M_Z$ interdependence, presented in Ref. [3], and to the effective mixing parameter $\sin^2\theta_{eff}^{lept}$ [4]. Moreover, in Ref. [4] the analysis of the $O(g^4 M_t^2/M_W^2)$ contributions to M_W and $\sin^2\theta_{eff}^{lept}$ was carried out in the $\overline{\mathrm{MS}}$ formulation of Ref. [5] as well as in two different implementations of the on-shell (OS) scheme [6]. It was shown that the inclusion of $O(g^4 M_t^2/M_W^2)$ effects sharply reduces the scheme and residual scale dependence of the theoretical predictions for M_W and $\sin^2\theta_{eff}^{lept}$, and suggests a comparable reduction of the overall theoretical uncertainty [7,8].

The aim of this paper is to go further in the study of the $O(g^4 M_t^2/M_W^2)$ corrections. Our purpose is actually manifold:

- First, we present the result of the calculation of the partial widths of the Z^0, Γ_f, for $f \neq b$, at $O(g^4 M_t^2/M_W^2)$ in both the $\overline{\mathrm{MS}}$ and OS schemes. As the case of the b quark involves a completely new class of vertex diagrams and would require a significant dedicated effort, it will not be considered here. We also study the scheme dependence of the results for the leptonic width, Γ_ℓ, finding it significantly reduced by the inclusion of the new contributions.

- We take the opportunity of the new result on the partial widths to describe some important aspects common to all $O(g^4 M_t^2/M_W^2)$ calculations which were not discussed in the preceding publications, in particular concerning the renormalization procedure and the Heavy Top Expansion (HTE) technique used in the calculations. We also provide some intermediate results and derivations in appendix A.

- Finally, we discuss some of the consequences of our results, in view of the present experimental situation. Following Ref. [7], we provide elementary interpolating formulas in different schemes for Γ_ℓ. For completeness, we also report and update the analogous formulae for M_W and $\sin^2\theta_{eff}^{lept}$.

A few topics relative to the $O(g^4 M_t^2/M_W^2)$ calculations were already covered in some detail in preceding related publications, and we will not dwell on them further. For instance, the impact of the new calculations on the indirect determination of M_H is quite important, and this has been extensively discussed in Refs. [4, 7–9]. Although we do not repeat this discussion here, we will use the interpolating formulae for M_W, $\sin^2\theta_{eff}^{lept}$, and Γ_ℓ, together with the latest experimental data, to obtain two new estimates for M_H. One is based on information coming only from precision measurements, while the other includes also the results of direct search experiments, using the method developed in Ref. [10].

The paper is organized as follows. In the next section we discuss some issues concerning the renormalization procedure we have followed. Section 3 deals with the technical matter of the HTE. In section 4 we present the analysis of the corrections to the Z partial widths to $O(g^4 M_t^2/M_W^2)$. Section 5 contains the interpolating formulae and our estimates for M_H. Finally, we present a brief summary. We also include two appendices. In appendix A we provide the two-loop W and Z^0 self-energies to $O(g^4 M_t^2/M_W^2)$, which may be useful in different contexts. Appendix B contains instead the explicit expressions of the $O(g^4 M_t^2/M_W^2)$ corrections to the various Z partial width form factors.

2 Renormalization

In this section we discuss some aspects of the $O(g^4 M_t^2/M_W^2)$ renormalization for processes involving four light fermions as external states. The main difference between the one and two-loop cases is that in the latter we also have to consider the renormalization of the unphysical sector. In the following, we first discuss the renormalization of the unphysical sector in a general way. We then explain why the use of OS masses for the vector bosons, rather than $\overline{\rm MS}$ mass parameters, is particularly useful in our calculations and illustrate different options for the renormalization of their unphysical counterparts.

As is well known, there are constraints that link the longitudinal component of the vector bosons, the corresponding pseudo-Goldstone bosons, and the Faddeev-Popov (FP) ghosts. In higher order calculations, it is convenient to choose a renormalization procedure that automatically respects the Slavnov-Taylor Identities (STI) which are induced by the local gauge invariance of the original Lagrangian before spontaneous symmetry breaking. According to the organization of the calculation, it is possible to use different procedures that respect the STI's and are particularly convenient in order, for instance, to minimize the number of diagrams to be considered. Of course, physical amplitudes are independent of the chosen procedure, and this can be used as an additional check of the calculation. For the problem at hand, the discussion can be kept at the one-loop level, and we can limit ourselves to contributions proportional to powers of M_t. In the following, we discuss only the W sector; the case of the Z^0 sector can be treated in a completely analogous manner, because the $\gamma - Z^0$ mixing does not contribute at the order of our calculation.

If we split the unrenormalized W polarization tensor into transverse and longitudinal

parts

$$\Pi_W^{\mu\nu}(q) = \left(g^{\mu\nu} - \frac{q^\mu q^\nu}{q^2}\right) A_{WW}(q^2) + \frac{q^\mu q^\nu}{q^2} \Pi^L_{WW}(q^2), \tag{1}$$

and we denote by $\Pi_{W\phi}$ the proper two-point function for the mixing between the W and its pseudo-Goldstone boson, ϕ, and by $\Pi_{\phi\phi}$ the self-energy of the latter, we obtain the following STI's in a general R_ξ gauge (see for ex. [11, 12])

$$\begin{aligned} &\xi \left[\Pi^L_{WW}(q^2) + M_Z \Pi_{W\phi}(q^2)\right] + G(q^2) = 0 \\ &q^2 \left[\Pi^L_{WW}(q^2) + 2 M_W \Pi_{W\phi}(q^2)\right] + M_W^2\, \Pi_{\phi\phi}(q^2) + M_W^2\, T = 0\,, \end{aligned} \tag{2}$$

where T represents the tadpole contribution and $G(q^2)$ is a term involving charged FP ghosts as external fields. Among other things, $G(q^2)$ contains the two-point function of the charged ghosts; as the ghost do not couple directly to fermions, at the one-loop level $G(q^2)$ is completely independent of the top quark.

We see that the first two terms of the second STI in Eqs. (2) vanish at $q^2 = 0$, and that therefore $\Pi_{\phi\phi}(0)$ is equal to the tadpole contribution. This uncovers the connection between the renormalization of the Goldstone boson mass and the one of the tadpole. In our calculation we employ the usual tadpole renormalization that minimizes the effective potential and consists in removing all tadpole graphs. This choice implies the subtraction of $\Pi_{\phi\phi}(0)$ from the two-point function of the pseudo-Goldstone boson [13, 14].

Concerning the longitudinal component of the two-point function of the W, we find it convenient to renormalize it in the same way as the transverse part, the one which is related to the mass counterterm. Therefore, the choice of the renormalized mass parameters employed in our analysis is going to affect the structure of the finite part of the counterterm in the unphysical sector. In practice, the choice is between the $\overline{\text{MS}}$ and OS mass definitions. For the other two-point functions appearing in Eq. (2) different options are possible, which all respect the STI's, and are equivalent at the level of physical amplitudes. They correspond to different ways of renormalizing the gauge-fixing parameters.

A first and very natural option (*heavy mass* procedure) consists in subtracting from each term in Eqs. (2) the contributions proportional to powers of M_t. In case an $\overline{\text{MS}}$ prescription for the vector boson masses is adopted, the subtraction applies only to the divergent part. This procedure is equivalent to a Taylor expansion in the external momentum and obviously respects the identities, as the unrenormalized self-energies do. We recall that $\Pi^L_{WW}(0) = A_{WW}(0) \approx \mathrm{Re}\, A_{WW}(M_W^2)$ at the order we are interested in, so that the OS mass counterterm corresponds to the first term of the Taylor expansion. There is a counterterm for the $W-\phi$ transition as well as for the $\phi^\pm$ two-point function, but the FP ghost self-energy needs not be renormalized, as it is independent of the top quark. In order to satisfy the second of Eqs. (2) at any q^2, a wave function renormalization Z_ϕ for the $\phi^\pm$ field is needed. On the other hand, $\phi^\pm$ appear only inside the loops in our calculations and the use of Z_ϕ is indeed not necessary. Therefore, we simply demand that the second of Eqs. (2) be satisfied at $q^2 = M_W^2$.

A second possibility consists in assigning no counterterm to the $W-\phi$ transition; this decreases the number of counterterms and simplifies their implementation. In fact, in the

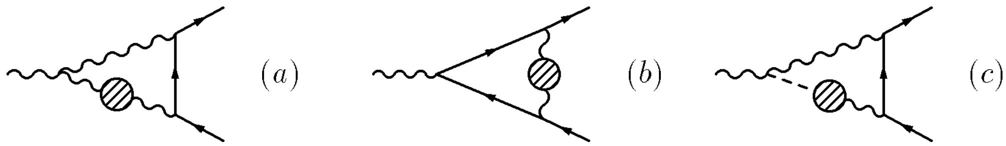

Figure 1: Two-loop vertex diagrams containing the top. Wavy (dashed) lines represent vector (scalar) bosons.

't Hooft-Feynman gauge it corresponds to renormalizing the masses of the vector boson and of the associated scalar boson and ghost in the same way (*bare gauge fixing*), apart from the supplementary subtraction at $q^2 = 0$, corresponding to the tadpole contribution, that we have discussed above. It therefore amounts to fix $\delta M_\phi^2 = \delta M_W^2 + T$ and $\delta M_c^2 = \delta M_W^2$ ($c^\pm$ are the FP ghosts) and is the closest to the naive parameter renormalization. Also this choice verifies both Eqs. (2) at $q^2 = M_W^2$, leaving room for a further arbitrary wave-function renormalization, which again can be avoided altogether.

We have explicitly verified that these two renormalization options (*heavy mass* and *bare gauge fixing*) are equivalent at the level of physical amplitudes in the cases at hand. Finally, we should mention that another possibility is the one presented in [15], which corresponds to the use of *renormalized gauge-fixing*.

For what concerns the three-point functions, we just recall that the renormalization of those couplings that contain masses is fixed by the Ward identities that link the Yukawa and bosonic coupling counterterm to the gauge coupling and mass renormalization.

From a technical point of view, the choice of OS masses as renormalized parameters, in particular for the W and Z^0 vector bosons, has some important advantages in the calculations considered here. The processes we are interested in always involve light external fermions and are mediated at lowest level (to excellent approximation) by gauge bosons only. In these cases, the two-loop box and vertex diagrams containing the top quark consist of a top-bottom insertion on a bosonic line belonging to a one-loop vertex (Fig.1a,b) or box[1], plus vertices that involve a $W - \phi$ transition, like the one shown in Fig.1c. Superficially, all these diagrams are either convergent or logarithmically divergent. However, they contain a quadratic subdivergence associated with the top-bottom loop insertions. If we employ the OS mass definition for the mass of the vector bosons, all the boxes and vertices involving insertions on vector boson lines can be neglected in the calculation because the associated mass counterterm graphs remove completely their M_t^2 dependence. Of course, this would not happen in the case of a pure $\overline{\rm MS}$ subtraction, as the remaining finite part would still be proportional to M_t^2.

The use of OS vector boson masses therefore absorbs a whole class of $O(g^4 M_t^2/M_W^2)$ diagrams and we have decided to present always our results in terms of OS masses for all the physical particles, also when we work in the $\overline{\rm MS}$ scheme. Indeed, this choice has some clear advantages even in the case the gauge couplings are renormalized in the $\overline{\rm MS}$ scheme [5, 16]: (i) it employs as mass parameters the physically measured masses

[1] A top loop vertex insertion on a trilinear coupling does not provide M_t^2 terms by dimensional reasons.

without introducing large radiative corrections in the coupling counterterms; (ii) it absorbs the large radiative corrections that appear in the one-loop relation between OS and $\overline{\rm MS}$ masses. Incidentally, one should also note that the conventional OS mass definition, identified by the counterterm $\mathrm{Re}\, A_{WW}(M_W^2)$, does not present any gauge ambiguity at the order of our calculations; as stressed in [17], this is not the case at $O(g^4)$ and beyond.

The *heavy mass* procedure that assigns a counterterm to the $W-\phi$ transition has an additional advantage: it allows us to neglect systematically all two-loop vertices and boxes in our calculations, including the diagrams of Fig.1c. In this case the only two-loop diagrams that we need to consider are two-point functions of the vector bosons: this is the approach followed in the present paper. If instead we work with *bare gauge fixing*, it should be apparent that only diagrams of the kind in Fig.1(a,b) will be removed at $O(g^4 M_t^2/M_W^2)$ after renormalization. The diagram of Fig.1(c) has to be explicitly calculated. However, as could be expected, its evaluation at $O(g^4 M_t^2/M_W^2)$ involves only self-energy integrals and therefore no additional difficulty is introduced. This approach was followed in Refs. [2, 3] and the detailed evaluation of the diagram of Fig.1(c) was discussed in Ref. [18][2].

3 Heavy top expansion of two-loop diagrams

In the preceding section we have seen that in the calculations at hand the only two-loop diagrams that need to be considered are two-point functions of the vector bosons, including the $\gamma - Z^0$ mixing for the calculation of the effective sine and the photon self-energy at vanishing momentum for the renormalization of the electric charge [6]. In this section we explain how we have evaluated these self-energy diagrams. We start motivating the choice of the next-to-leading order (NLO) HTE instead of a numerical computation, proceed to consider the classes of diagrams that need to be computed, and conclude discussing the quality of the approximation.

There are arguments [22] that two-loop self-energy integrals with arbitrary masses and momentum transfer cannot be expressed in terms of known elementary functions like polylogarithms. Although an analytic solution seems in the general case impossible, there exist several methods that permit an efficient numerical evaluation [23]. On the other hand, compact analytic results are available in a number of special cases, which apply to a variety of physical situations like small and large momentum expansions. The clear advantage of the analytic evaluation in a situation where at least one of the parameters, namely M_H, is largely unconstrained, is that the results can be readily implemented in

[2]Independently of the renormalization of the unphysical sector, vertex diagrams of the kind shown in Fig.1(c) can be excluded by the choice of a non-linear gauge fixing; for example the $\gamma W^{\pm}\phi^{\mp}$ coupling, which is characteristic of the R_ξ gauge, can be avoided, so that the photon separately couples to W and charged Goldstone bosons [19]. Consequent modifications [20] in the Faddeev-Popov sector of the SM do not affect the calculation, as ghosts do not couple to fermions. In the case of the photon vertex, also the background field gauge can be used to the same effect. Alternatively, it is possible to fix the gauge in such a way that the $Z^0 W^{\pm}\phi^{\mp}$ vertex is avoided [21].

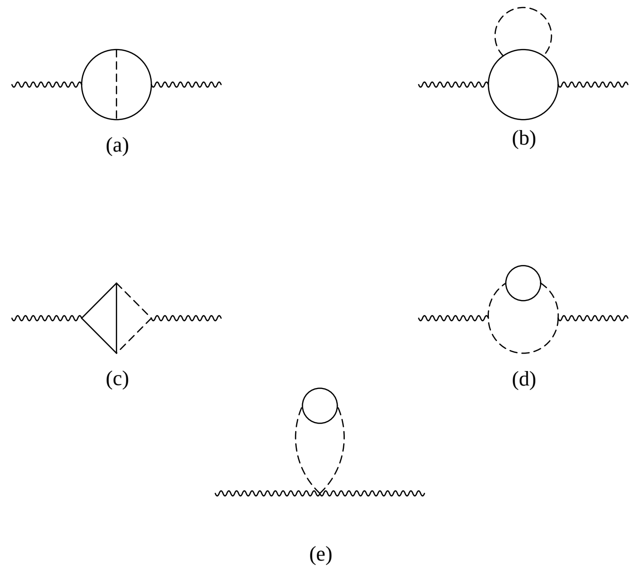

Figure 2: Two-loop topologies for vector boson self-energies. Dashed (solid) lines represent virtual bosons (fermions).

fitting routines. Furthermore, if one chooses to perform a numerical calculation at the two-loop level in the electroweak theory without any approximation, several challenging problems arise, like the very large number of diagrams, the implementation of the complete two-loop renormalization of the SM, etc. Therefore, following the conclusions of [1,2], our strategy has been to use a heavy mass expansion up to $O(g^4 M_t^2/M_W^2)$.

We have performed the calculations in the 't Hooft-Feynman gauge, where $M_\phi = M_c = M_W$. This choice proves to be convenient also in the evaluation of the integrals, as it limits the number of different mass scales occurring in each diagram. Concerning the bottom mass, we have set it to zero from the start. We have neglected all flavor violation. All two-loop self-energy diagrams containing the top have to be considered. The topologies are displayed in Fig.2. The subset of diagrams containing only scalar bosons in addition to the top and the bottom quarks is responsible for the leading $O(g^4 M_t^4/M_W^4)$ correction [24].

We distinguish between three classes of diagrams: (i) the ones for which a naive Taylor expansion in q^2 can be used because no light mass threshold is involved; (ii) those containing at least one bottom quark threshold, which we regard as zero mass threshold; (iii) those with at least one physical threshold of the order of the W mass (e.g. it can be $4M_W^2$, M_W^2, $(M_W + M_Z)^2$). Clearly, the two last classes of diagrams overlap (see for ex. the diagram in Fig. 2(c) where the fermion loop consists of two bottom and one top lines and the bosonic lines represent two W bosons). With respect to this classification of diagrams, the fact that the Higgs boson mass is *a priori* arbitrary implies that we have to consider two scenarios: (a) the case in which M_H is light compared to the top mass, namely $M_H \approx M_W$ and therefore $M_H \ll M_t$; (b) the case in which M_H is considered heavy compared to M_W, and the heavy mass expansion is implemented leaving the ratio between M_H and M_t finite and arbitrary. For most diagrams containing the Higgs, the HTE provides different expressions in the two cases. This explains why in app. A the

expressions for the W and Z^0 self-energies are given in the two regimes.

In the case of class (i) diagrams we adopt a Taylor expansion first in the small external momentum and then in the light masses keeping only terms proportional to powers of M_t. The Taylor expansion of the two-loop integrals is viable for values of q^2 up to the first physical threshold. Since in our calculations $q^2 = M^2_{W,Z}$ or 0, it follows that $q^2 \ll M_t^2$ and this procedure is justified for class (i). Typical diagrams belonging to this class are

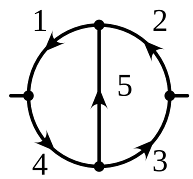

Figure 3: Two-loop master self-energy diagram.

those of Fig.2(a) where the fermion in the loop is a top quark. Referring to the two-loop master diagram of Fig.3, any diagram containing a heavy particle (top and possibly Higgs boson) in place 1 *and* 2 can be safely included in this class. In practice, the q^2 expansion is implemented using (k and m generically indicate one momentum of integration and one internal mass)

$$\frac{1}{(k+q)^2 - m^2} \to \sum_{n=0}^{\infty} (-1)^n \frac{(2k \cdot q + q^2)^n}{(k^2 - m^2)^{n+1}} \tag{3}$$

under the n-dimensional integral. For arbitrary internal masses, the two-loop integrals at zero momentum transfer can be expressed as a combination of logarithms and dilogarithms [25]. Therefore, we reduce the integrand to scalar vacuum integrals and for the evaluation of the integrals with higher powers of the propagators we follow the iterative method of first paper in [25].

For the diagrams of class (ii) the Taylor expansion is bound to fail because it cannot describe the physical threshold at $q^2 = 0$. The typical diagram has bottom at place 1 and 4 and top at place 2 and 3 in Fig. 3. The simple replacement of Eq. (3) when $m = 0$ leads to increasingly severe infrared divergences for increasing n. Heavy mass or small momentum expansions in these cases are therefore asymptotic expansions, about which a rich technical literature exists [26]. An elegant algorithm to implement the asymptotic expansion in dimensional regularization has been developed in Ref. [26] and applied to this class of diagrams in [27]. The technique we have used, however, is based on the repeated application of the identity

$$\frac{1}{(k_1+k_2)^2 - M^2} = \frac{1}{k_1^2 - M^2} - \frac{k_2^2 + 2k_1 \cdot k_2}{[(k_1+k_2)^2 - M^2](k_1^2 - M^2)} \tag{4}$$

where M is a heavy mass and $k_{1,2}$ are the integration momenta. The first term on the r.h.s. of Eq. (4) leads to a disconnected integral (product of two one-loop integrals) that can be evaluated exactly, i.e. for arbitrary q^2, and contains $\ln q^2$ terms that describe the physical threshold. The second term, instead, leads to a two-loop integral with improved

infrared convergence in the k_2 integration and improved ultraviolet convergence in the k_1 integration. Therefore, if, for example, the original integral is IR logarithmically divergent in the k_2 integration when $q \to 0$, the corresponding two-loop integral associated with the second term in Eq. (4) evaluated at $q^2 = 0$ gives a finite result that differs from the complete result for arbitrary q^2 by terms $O(q^2/M^2 \ln(q^2/M^2))$. In case of integrals more seriously IR divergent, an iterative use of Eq. (4) gives an approximate evaluation, up to terms suppressed by the heavy mass, through a combination of integrals (a set of disconnected ones plus two-loop integrals evaluated at $q^2 = 0$) whose analytic expressions are known. Thus, one can combine the expansion (3) with the repeated use of Eq. (4) to obtain the asymptotic expansion of the original integral at the desired order. Indeed, at each step of the expansion the more serious IR divergent behavior introduced by (3) can be balanced by the convergent IR factor from the second term of Eq. (4), while the part associated with the first term in Eq. (4) can be always evaluated exactly. An explicit example of the application of this method has been provided in [18]. We have checked that our results coincide with those of Ref. [27] in all the cases relevant to the present calculation.

The class (iii) diagrams differs from those of class (ii) because the threshold is not at $q^2 = 0$ and can in fact be well above the q^2 at which the integrals are evaluated. Nevertheless, the Taylor expansion cannot be employed here because we are interested in the HTE and not in the small momentum expansion. Therefore, in order to extract all the terms enhanced by powers of M_t, one has to use the same procedure adopted for case (ii), reducing the original integral to a sum of disconnected ones, to be evaluated exactly keeping the light masses (M_W, M_Z and possibly M_H) and the q^2, plus two-loop connected integrals with $q^2 = 0$ which have to expanded in powers of M_t^2. The disconnected diagrams are responsible for the terms containing the functions $B_0[q^2, m_1^2, m_2^2]$ in the two-loop self-energies of app. A. Also in this case we have checked our results against the relevant existing literature [28].

A crucial question is now whether the approximation based on the NLO HTE described above is reliable. The second term $O(g^4 M_t^2/M_W^2)$ of the two-loop HTE seems to be quite important wrt the first [3], so the convergence of the HTE may be legitimately questioned. An important point to take into account in this respect is that this is true mainly for a light Higgs, where the approximation of keeping $M_W = 0$ and $M_H \neq 0$ manifestly fails. The result of [24], which was based on such approximation, becomes meaningless in this regime, and no hierarchy among the first and the second term of the asymptotic expansion should be expected. Moreover, we know from Ref. [4] that the size of the $O(g^4 M_t^2/M_W^2)$ contributions to $\sin^2 \theta_{eff}^{lept}$ and M_W depends very strongly on the scheme adopted. This tells us that reducible contributions (products of one-loop integrals) are very important there. Since we know that the HTE works very well at one-loop level where the leading quadratic term is dominant, the reducible contribution is well approximated by the first two terms of the HTE. Concerning the irreducible contributions, the present two-loop calculations are based on two-point functions only. Unlike the case of three and four point-functions [29], the HTE appears to work quite well for self-energies, as has been demonstrated in the case of QCD corrections up to three loops in the second paper of

Ref. [38]. Ultimately, however, the most convincing evidence on the quality of the NLO HTE approximation comes *a posteriori* from the sharp reduction of the scheme and scale dependence of the predictions for M_W, $\sin^2\theta_{eff}^{lept}$, and, as will be seen later, Γ_ℓ.

A conclusive test of our approximation can only come from a comparison of the HTE with a two-loop numerical calculation. A first partial test of the HTE [31] for the two-loop electroweak corrections has been obtained by comparing the results of [3,4] with the calculation of Ref. [30] by Bauberger and Weiglein. They calculated the two-loop self-energies which contain the Higgs boson together with fermions through a direct numerical evaluation of Feynman diagrams, without any heavy mass expansion. Although this is only a subset of the diagrams involving the Higgs boson, the result can be used as a partial test of the HTE employed here, because it includes all the diagrams containing both top and Higgs. The Higgs mass dependences of the predictions for M_W and $\sin^2\theta_{eff}^{lept}$ according to Refs. [4] and [30] have been accurately compared in [8, 31]. Very small deviations appear to be attributable to the use of the HTE, of the order of 1 MeV and 10^{-5} for M_W and $\sin^2\theta_{eff}^{lept}$, respectively. Such deviations are well within the range of theoretical errors estimated from scheme and scale dependence [4, 8].

4 The Z^0 decay partial widths

This section contains the main result of the paper, namely the $O(g^4M_t^2/M_W^2)$ corrections to the partial decay widths $Z \to f\bar{f}$, Γ_f, of the Z^0 boson. The only case which is not covered is the one of final b-quarks, because it involves specific $O(g^4M_t^2/M_W^2)$ vertex corrections. As in our previous calculations [3,4], we first derive the result in the $\overline{\mathrm{MS}}$ framework of Ref. [5] and then discuss the scheme dependence by considering the analogous contributions in two implementations of the OS scheme.

We recall that the formulation of Ref. [5] employs $\overline{\mathrm{MS}}$ couplings evaluated at the scale M_Z while using OS masses for the physical particles. In particular, the coupling constants of the SU(2) and U(1) groups are written in terms of $\hat{e}^2 = e^2/(1+2\,\delta e/e)_{\overline{\mathrm{MS}}}$, the $\overline{\mathrm{MS}}$ electromagnetic coupling, and $\sin^2\hat{\theta}_W(M_Z) \equiv \hat{s}^2$, the $\overline{\mathrm{MS}}$ electroweak mixing parameter. Even though the top quark is heavier than the Z^0 mass scale, it is not decoupled in the definition of the $\overline{\mathrm{MS}}$ couplings, according to the convention of Ref. [5]. The subscript $\overline{\mathrm{MS}}$ in the charge renormalization counterterm $(2\,\delta e/e)$ indicates the pole subtraction, a notation that will also be used henceforth. Although the t'Hooft scale μ is conventionally set equal to M_Z, in our calculations we leave it unspecified. This allows us to study the scale dependence of the results. In this framework, M_W and the renormalized parameter $\hat{s}^2$ are calculated from G_μ, α, and M_Z through the two relations $(\hat{c}^2 = 1-\hat{s}^2)$

$$\frac{M_W^2}{M_Z^2} = \frac{\hat{c}^2}{1-\frac{\hat{e}^2}{\hat{s}^2}\Delta\hat{\rho}}, \qquad \hat{s}^2 = \frac{\pi\alpha}{\sqrt{2}G_\mu M_W^2(1-\Delta\hat{r}_W)}. \tag{5}$$

The $O(g^4M_t^2/M_W^2)$ contributions to the radiative corrections $\frac{\hat{e}^2}{\hat{s}^2}\Delta\hat{\rho}$ and $\Delta\hat{r}_W$ were discussed in Refs. [3, 4]. In appendix B we report the explicit expression for the $O(g^4M_t^2/M_W^2)$

contribution to $(2\,\delta e/e)_{\overline{\rm MS}}$. We notice that there is a technical advantage in using $\overline{\rm MS}$ couplings. Indeed, the associated one-loop counterterms, $\delta^{(1)}\hat{e}$ and $\delta^{(1)}\hat{s}^2$, are pure poles that do not contain any M_t^2 dependence and this reduces the number of counterterm diagrams to be considered.

The amplitude for the decay of a Z^0 boson into two fermions f can be expressed in the $\overline{\rm MS}$ scheme as [32]

$$M_Z^\mu = -i\frac{\hat{e}}{\hat{s}\hat{c}}\sqrt{\hat{\eta}_f}\,\langle f\bar{f}|\,\frac{1}{2}J_3^\mu - \hat{s}^2\,\hat{k}_f(M_Z^2)\,J_\gamma^\mu\,|0\rangle, \tag{6}$$

where J_3^μ is the $SU(2)$ neutral current and J_γ^μ is the photonic current[3]. The corresponding expression for the partial width $Z\to f\bar{f}$ is therefore

$$\Gamma_f = N_c^f\,\frac{\hat{e}^2}{\hat{s}^2\hat{c}^2}\frac{M_Z}{96\pi}|\hat{\eta}_f|\left\{1-4\,I_f^3\,Q_f\,\hat{s}^2{\rm Re}\hat{k}_f + 8\,Q_f^2\,\hat{s}^4|\hat{k}_f|^2\right\} + O(m_f^2/M_Z^2), \tag{7}$$

where N_c^f is the color factor for the fermion f, $I_f^3 = \pm 1$ its isospin quantum number, Q_f its electric charge, and the appropriate QED and QCD corrections have not been explicitly indicated.

The $O(g^4M_t^2/M_W^2)$ corrections to $\hat{k}_f(M_Z^2)$ have been already considered in Refs. [4,18]. In the $\overline{\rm MS}$ scheme they are universal (with the exception of the b final state) because they can be entirely expressed in terms of the $\gamma - Z$ self-energy, as a consequence of the discussion in Sec.2. The overall factor $\hat{\eta}_f$ can be expressed as $\hat{\eta}_f = 1 + (\hat{e}^2/\hat{s}^2)(\Delta\hat{\eta}_f^{(1)} + \Delta\hat{\eta}_f^{(2)})$, where the one-loop contribution is given by

$$(\hat{e}^2/\hat{s}^2)\Delta\hat{\eta}_f^{(1)} = {\rm Re}A_{ZZ}^{(1)'}(M_Z^2)\Big|_{\overline{\rm MS}} + \frac{\hat{g}^2}{16\pi^2}\bar{V}_{ff}(M_Z^2)\Bigg|_{\overline{\rm MS}}. \tag{8}$$

The function $\bar{V}_{ff}(M_Z^2)$ is defined in Eq. (12d) of Ref. [32] and ${\rm Re}A_{ZZ}^{'(1)}(M_Z^2)$ is given in the appendix of the same paper.

In analogy to the case of $\hat{k}_f$, the $\overline{\rm MS}$ two-loop $O(g^4M_t^2/M_W^2)$ contribution $\Delta\hat{\eta}_f^{(2)}$ is the same for all light fermions with the exception of the bottom. Indeed, we have seen in Sec.2 that one can choose a suitable renormalization of the unphysical sector (*heavy mass* procedure) which avoids the appearance of two-loop vertices at this order of the calculation. In this case $\Delta\hat{\eta}_f^{(2)}$ is given exclusively by the two-loop wave function renormalization factor of the Z^0 boson

$$\Delta\hat{\eta}_f^{(2)} \equiv \Delta\hat{\eta}^{(2)} = {\rm Re}A_{ZZ}^{'(2)}(M_Z^2)\Big|_{\overline{\rm MS}}\quad . \tag{9}$$

We recall that the one-loop correction $\Delta\hat{\eta}_f^{(1)}$ and the one-loop $\overline{\rm MS}$ coupling counterterms do not contain M_t^2 terms. Therefore $\Delta\hat{\eta}_f^{(2)}$ can be directly obtained from the irreducible diagrams contributing to the two-loop self-energy of the Z^0 plus the mass counterterm graphs. In appendix A the sum of these two contributions to $A_{ZZ}^{(2)}(q^2)$ is presented. The

[3]In Ref. [32] the correction $\hat{\eta}_f$ is indicated as $\bar{\rho}_{ff}$.

explicit expression of $\Delta\hat{\eta}^{(2)}$ for arbitrary μ can be obtained differentiating Eqs. (A3,A4) with respect to q^2 and is reported in Eq. (B1) (for the case $M_H \ll M_t$) and Eq. (B2) ($M_H \gg M_W$) of appendix B. Numerically, $\Delta\hat{\eta}^{(2)}$ is small in all the relevant range of M_H and M_t values. For $M_t = 175$ GeV, $\mu = M_Z$, and $\hat{s}^2 = 0.2315$, $\Delta\hat{\eta}^{(2)}$ amounts to 7×10^{-5} at $M_H = 50$ GeV and decreases almost monotonically for larger M_H. The two expressions for light and heavy Higgs match very well around $M_H = 96$ GeV, where they reach 3×10^{-5}. In the range 200 GeV $\lesssim M_H \lesssim$ 1 TeV, $\Delta\hat{\eta}^{(2)}$ is always less than 2×10^{-5}.

We consider now the Z^0 partial widths in the OS scheme. To derive the relevant expressions we follow the same steps and employ the same notation as in Ref. [4]. The idea is to use the known one-loop relations between the $\overline{\text{MS}}$ and OS schemes [5] in order to translate the $\overline{\text{MS}}$ quantities $\hat{e}$ and $\hat{s}$ appearing in Eq. (7) into OS parameters. Following Ref. [4], we write

$$\hat{e}^2/\hat{s}^2 = (G_\mu/\sqrt{2})8M_W^2[1-(\hat{e}^2/\hat{s}^2)\hat{f}\,], \tag{10}$$

$$\hat{s}^2/s^2 = 1 + (c^2/s^2)(\hat{e}^2/\hat{s}^2)\;\Delta\hat{\rho}, \tag{11}$$

where $s^2 = 1 - c^2$ is an abbreviation for $\sin^2\theta_W \equiv 1 - M_W^2/M_Z^2$ and

$$\hat{f} = \Big[(\mathrm{Re}A_{WW}(M_W^2) - A_{WW}(0))/M_W^2 + V_W + M_W^2 B_W\Big]_{\overline{\text{MS}}}, \tag{12}$$

$$\Delta\hat{\rho} = \mathrm{Re}\,\Big[A_{WW}(M_W^2) - \hat{c}^2 A_{ZZ}(M_Z^2)\Big]_{\overline{\text{MS}}}/M_W^2 \quad . \tag{13}$$

In these expressions $A_{WW}(q^2)$ and $A_{ZZ}(q^2)$ are the transverse W and Z^0 self-energies [5, 6, 34] with $\hat{e}^2/\hat{s}^2$ factored out[4]. Similarly, a factor $\hat{e}^2/\hat{s}^2$ has been extracted from the definition of $\Delta\hat{\rho}$ and $\hat{f}$. The term $V_W + M_W^2 B_W$ in Eq. (12) represents vertex and box diagram contributions to the μ decay, modulo a factor $e^2/\hat{s}^2$ [6]. The quantities $\hat{f}$ and $\Delta\hat{\rho}$ are actually functions of $\hat{s}^2$. Iterating Eqs. (10) and (11) we can express $\hat{e}^2/\hat{s}^2$ and $\hat{s}^2$ completely in terms of G_μ and s^2. We note from Eq. (11) that $\hat{s}^2 - s^2 = c^2(\hat{e}^2/\hat{s}^2)\Delta\hat{\rho} \approx 3\,c^2\,x_t + ...$ where $x_t = G_\mu M_t^2/8\pi^2\sqrt{2}$ and the ellipses represent subleading contributions. Thus, the replacement $\hat{s}^2 = s^2\,[1 + (c^2/s^2)\,3\,x_t + ...]$ in the one-loop components of $\hat{f}(\hat{s}^2)$ and $\Delta\hat{\rho}(\hat{s}^2)$ induces additional contributions of $O(g^4 M_t^2/M_W^2)$.

We recall that in Ref. [4] two ways of writing the OS corrections Δr [6] and k [34] were discussed. The two formulations are equivalent to $O(g^4M_t^2/M_W^2)$ but include in different ways higher orders effects. The first one, indicated as OSI, generalizes the Consoli Hollik Jegerlehner formula [35] for Δr to $O(g^4M_t^2/M_W^2)$ by writing

$$1 - \Delta r = \left(1 + \frac{2\delta e}{e}\bigg|_{\overline{\text{MS}}} - \frac{e^2}{s^2}\bar{f}(s^2)\right)\left(1 + \frac{c^2}{s^2}\frac{8M_W^2 G_\mu}{\sqrt{2}}\Delta\bar{\rho}(s^2)\right), \tag{14}$$

where $\bar{f}(s^2)$ and $\Delta\bar{\rho}(s^2)$ are the OS counterparts of Eqs. (12) and (13) and are defined in appendix B. Eq. (14) shows a structure for Δr that is very close to that obtained in the

[4]We have excluded a factor $(A_{\gamma Z}(M_Z^2))^2$ from the Z^0 mass counterterm because it does not contribute at the order of the calculation. In the numerics, however, the square of the imaginary part is not negligible because of the additive contribution of all the light fermions, is gauge independent, and is enhanced by a factor π^2. As in the case of the effective sine [33], we have included it in our numerical studies.

$\overline{\rm MS}$ framework [5]. As the $\overline{\rm MS}$ formulation automatically resums reducible contribution and therefore includes part of higher order corrections, Eq. (14) provides an analogous resummation formula in the OS scheme. Moreover, similarly to $\overline{\rm MS}$, Eq. (14) contains some residual μ-dependence at $O(g^4)$.

A similar analysis can be performed for the Z^0 partial widths. Referring to Eq. (7), we note that the OS analogue k_f of the form factor $\hat{k}_f$ depends on the fermion f, unlike its $\overline{\rm MS}$ counterpart. In Ref. [4] k_f has been presented only for a leptonic final state. In appendix B we generalize this result to the case of arbitrary fermion but the b quark. We still have to discuss the translation of the prefactor into the OS language. Indeed, we can rewrite $\frac{\hat{e}^2}{\hat{s}^2\hat{c}^2}|\hat{\eta}_f|$ in Eq. (7) in terms of OS quantities keeping terms up to $O(g^4 M_t^2/M_W^2)$ and also try to resum some higher order effect, in analogy to the $\overline{\rm MS}$ scheme. Using Eqs. (10) and (11), we obtain

$$\frac{\hat{e}^2}{\hat{s}^2\hat{c}^2}|\hat{\eta}_f| \ \stackrel{OSI}{\longrightarrow}\ 4\sqrt{2}G_\mu M_Z^2 \frac{\left|1+\frac{8G_\mu M_W^2}{\sqrt{2}}\Delta\bar{\eta}_f(s^2)\right|}{1-\frac{8G_\mu M_W^2}{\sqrt{2}}\left(\Delta\bar{\rho}(s^2)-\bar{f}(s^2)\right)}, \tag{15}$$

where

$$\Delta\bar{\eta}_f(s^2) = \Delta\hat{\eta}_f^{(1)}(s^2) + \Delta\bar{\eta}_f^{(2)}(s^2) \tag{16}$$

with

$$\Delta\bar{\eta}_f^{(2)}(s^2) = \Delta\hat{\eta}_f^{(2)}(s^2) + \Delta\bar{\eta}_{f,add}^{(2)}(s^2) \ \ . \tag{17}$$

In the spirit of the OSI scheme, Eq. (15) follows closely the $\overline{\rm MS}$ formulation, implies some resummation, and is actually μ-dependent at $O(g^4)$. Therefore, we adopt Eq. (15) whenever we employ OSI to calculate s^2. Explicitly, $\Delta\hat{\eta}_f^{(1)}(s^2)$ is the one-loop OS result with the overall coupling written in terms of G_μ, $\Delta\hat{\eta}_f^{(2)}(s^2)$ is given by Eqs. (B1) and (B2) in which $\hat{s}^2$ has been replaced by s^2, while $\Delta\bar{\eta}_{f,add}^{(2)}$ is the term induced by the shifts $\hat{s}^2 \to s^2$ in the one-loop result and it is provided in appendix B.

In the second implementation of the OS scheme introduced in Ref. [4], called OSII, Δr contains only the two-loop contributions proportional to M_t^4 and M_t^2, without any $\overline{\rm MS}$-like resummation, and it is strictly μ independent. In this case

$$\Delta r = \Delta r^{(1)} + \Delta r^{(2)} + \left(\frac{c^2}{s^2}\right)^2 N_c\, x_t \left(2\frac{e^2}{s^2}\Delta\bar{\rho}^{(1)} - N_c \frac{\alpha}{16\pi\, s^2}\frac{M_t^2}{M_W^2}\right), \tag{18}$$

where $\Delta r^{(1)}$ is the original one-loop OS result of Refs. [6,34], expressed in terms of α and s^2, $\Delta r^{(2)} = (e^2/s^2)\bar{f}^{(2)} - (c^2/s^2)(e^2/s^2)\Delta\bar{\rho}^{(2)}$. The last term in Eq. (18) represents higher order reducible contributions induced by resummation of one-loop corrections, while $\Delta r^{(2)}$ contains the corresponding irreducible components. In the same spirit of what has been done for Δr in the OSII formulation, we now consider a different way to write the prefactor $\frac{\hat{e}^2}{\hat{s}^2\hat{c}^2}|\hat{\eta}_f|$ in the OS scheme. We expand the r.h.s of Eq. (15) and retain only two-loop effects enhanced by powers of M_t, obtaining a μ-independent result:

$$\frac{\hat{e}^2}{\hat{s}^2\hat{c}^2}|\hat{\eta}_f| \ \stackrel{OSII}{\longrightarrow}\ \frac{8G_\mu M_Z^2}{\sqrt{2}}\Bigg[1+\frac{8G_\mu M_W^2}{\sqrt{2}}\left(\Delta\bar{\eta}_f - \bar{f} + \Delta\bar{\rho}\right)$$

	Γ_ℓ(MeV)		
M_H	OSI	OSII	$\overline{\rm MS}$
65	84.030	84.028	84.029
100	84.014	84.012	84.013
300	83.926	83.922	83.925
600	83.849	83.845	83.849
1000	83.791	83.786	83.791

Table 1: Predicted values of Γ_ℓ in OSI, OSII, and $\overline{\rm MS}$. QCD corrections based on μ_t-parametrization optimized. $M_t = 175$GeV, $\alpha_s(M_z) = 0.118$, $\Delta\alpha_{had} = 0.0280$,$M_z = 91.1863$.

	Γ_ℓ(MeV)		
M_H	OSI	OSII	$\overline{\rm MS}$
65	84.051	84.062	84.044
100	84.035	84.045	84.028
300	83.942	83.949	83.937
600	83.862	83.867	83.858
1000	83.801	83.804	83.797

Table 2: As in Table 1, but excluding $O(g^4 M_t^2/M_W^2)$ corrections.

$$+ \frac{8 G_\mu M_W^2}{\sqrt{2}} N_c x_t \left(2\Delta\bar{\rho}^{(1)} + \Delta\bar{\eta}_f^{(1)} - 2\bar{f}^{(1)} \right) - N_c^2 x_t^2 \Big] \quad . \tag{19}$$

The two OS approaches that we have introduced are equivalent at $O(g^4 M_t^2/M_W^2)$ but differ by $O(g^4)$ and higher order terms. Together with the $\overline{\rm MS}$ scheme, they provide us with a broad spectrum of possibilities to study the scheme dependence of our results. Summarizing our discussion of the OS scheme, we write Eq. (7) as

$$\Gamma_f = N_c^f \frac{M_Z}{96\pi} P \left\{ 1 - 4 I_f^3 Q_f s^2 \mathrm{Re} k_f + 8 Q_f^2 s^4 |k_f|^2 \right\} + O(m_f^2/M_Z^2), \tag{20}$$

where we evaluate the various terms in two different ways: (i) in the OSI approach the prefactor P is given by r.h.s of Eq. (15), while the OS sine is computed from α, G_μ and M_Z using Δr from Eq. (14). The k_f employed is accordingly given by Eq.(16) of Ref. [4]. (ii) in the OSII scheme, instead, the result is obtained using Eq. (19) for P, Δr given by Eq. (18), and the factor k_f given by Eq.(17) of Ref. [4].

Tables 1 and 2 present numerical results for the leptonic width of the Z^0, Γ_ℓ, after and before the inclusion of the $O(g^4 M_t^2/M_W^2)$ contributions. These tables are the analogue

for Γ_ℓ of the corresponding tables of [4] for M_W and $\sin^2\theta_{eff}^{lept}$. We have used exactly the same inputs of that paper and employed the same procedure in deriving the numerical results. We have neglected all final state mass effects. The two-loop [36, 37] and leading three-loop [38] QCD corrections are calculated according to the μ_t parametrization [4], a procedure of implementing the QCD corrections in which the pole top-quark mass M_t is expressed in terms of $\hat{m}_t(\mu_t) = \mu_t$, the $\overline{\rm MS}$-parameter, leading to sharply reduced QCD effects, and μ_t/M_t is evaluated by optimization methods [39]. We have verified that the conventional implementation of the QCD corrections in terms of the top pole mass leads to very close results, within 4 KeV at most. From Tables 1 and 2 we see that the scheme dependence of the results is strongly decreased by the inclusion of the $O(g^4 M_t^2/M_W^2)$ contributions, a pattern that was already observed for M_W and $\sin^2\theta_{eff}^{lept}$ in Ref. [4]. In particular, we find a maximal variation of 5 KeV in Table 1, compared to 18 KeV in Table 2. A reasonable estimate of the theoretical uncertainty due to uncalculated electroweak effects is therefore $O(5)$ KeV. Adding the QCD uncertainty, estimated to be ≈ 7 KeV in [8], there is good agreement with the results in Table 10 of the second paper in [40]. We also observe good agreement between this last reference and the error estimates for M_W and $\sin^2\theta_{eff}^{lept}$ presented in [4, 8]. In the case of the leptonic widths, however, the impact of these corrections (at most 34 KeV) remains in all schemes well below the present experimental error of 90 KeV (assuming lepton universality). We have also observed a reduction of the scale dependence of the Γ_ℓ prediction in the $\overline{\rm MS}$ and in the OSI scheme when the $O(g^4 M_t^2/M_W^2)$ contributions are included.

5 Discussion

The results of the $O(g^4 M_t^2/M_W^2)$ calculations, together with all relevant $O(\alpha\alpha_s)$ [36] and the leading $O(\alpha\alpha_s^2)$ QCD corrections [38], can be summarized by very simple interpolating formulas. Indeed, the relative uncertainty of most of the input parameters is quite small and their effect on the observables can be easily linearized, with the only exception of the Higgs mass. In Ref. [7] formulae for $\sin^2\theta_{eff}^{lept}$ and M_W as functions of M_H, M_t, α_s and the hadronic contribution to the running of the electromagnetic coupling have been presented for the three different electroweak schemes introduced in the previous sections, namely $\overline{\rm MS}$, OSI, and OSII. Here we apply the same procedure to the case of Γ_ℓ and slightly update the results for M_W and $\sin^2\theta_{eff}^{lept}$. The only differences with respect to Ref. [7] are that here we employ (i) the new value $G_\mu = 1.16637 \times 10^{-5}$ GeV^{-2} obtained after incorporation of the complete two-loop QED corrections to the muon decay [41] and (ii) the new central value $M_Z = 91.1867$ GeV. These two changes in the inputs amount to a very small shift of the overall normalization, common to the three schemes. The analytic formulae are of the form

$$\sin^2\theta_{eff}^{lept} = (\sin^2\theta_{eff}^{lept})_0 + c_1\,A_1 + c_2\,A_2 - c_3\,A_3 + c_4\,A_4, \tag{21}$$

$$M_W = M_W^0 - d_1\,A_1 - d_5\,A_1^2 - d_2\,A_2 + d_3\,A_3 - d_4\,A_4, \tag{22}$$

$$\Gamma_\ell = \Gamma_\ell^0 - g_1\,A_1 - g_5\,A_1^2 - g_2\,A_2 + g_3\,A_3 - g_4\,A_4, \tag{23}$$

Scheme	$(\sin^2\theta_{eff}^{lept})_0$	$10^4 c_1$	$10^3 c_2$	$10^3 c_3$	$10^4 c_4$
$\overline{\rm MS}$	0.231513	5.23	9.86	2.78	4.5
OSI	0.231527	5.19	9.86	2.77	4.5
OSII	0.231543	5.26	9.86	2.68	4.4

Table 3: Values of $(\sin^2\theta_{eff}^{lept})_0$ and c_i in Eq. (21) for three electroweak schemes that incorporate $O(g^4 M_t^2/M_W^2)$ corrections in the μ_t-parametrization of QCD corrections [2].

Scheme	M_W^0	$10^2 d_1$	$10\, d_2$	$10\, d_3$	$10^2 d_4$	$10^3 d_5$
$\overline{\rm MS}$	80.3829	5.79	5.17	5.43	8.5	8.0
OSI	80.3809	5.73	5.18	5.41	8.5	8.0
OSII	80.3807	5.81	5.18	5.37	8.5	7.8

Table 4: Values of M_W^0 and d_i in Eq. (22), in GeV, as in Table 3.

where

$$A_1 = \ln\frac{M_H}{100\ \mathrm{GeV}}, \qquad A_2 = \frac{(\Delta\alpha)_h}{0.0280} - 1,$$
$$A_3 = \left(\frac{M_t}{175\ \mathrm{GeV}}\right)^2 - 1, \qquad A_4 = \frac{\alpha_s(M_Z)}{0.118} - 1,$$

$(\Delta\alpha)_h$ is the five-flavor hadronic contribution to the QED vacuum-polarization function at $q^2 = M_Z^2$, and $(\sin^2\theta_{eff}^{lept})_0$, M_W^0, and Γ_ℓ^0 are (to excellent approximation) the theoretical results at the reference point $M_H = 100$ GeV, $(\Delta\alpha)_h = 0.0280$, $M_t = 175$ GeV, and $\alpha_s(M_Z) = 0.118$. The values of $(\sin^2\theta_{eff}^{lept})_0$, M_W^0, Γ_ℓ^0, c_i (i =1-4) and d_j, g_j (j =1-5) for the three electroweak schemes of Ref. [4] are given in Tables 3-5. We present the coefficients in the case of the μ_t-parametrization mentioned in the previous section, which was shown in Ref. [4] to give results very close to the more conventional parametrization in terms of the top pole mass. These formulae are very accurate for $75 \lesssim M_H \lesssim 350$ GeV with the other parameters in the ranges $170 \lesssim M_t \lesssim 181$ GeV, $0.0273 \lesssim \Delta\alpha_h \lesssim 0.0287$, $0.113 \lesssim \alpha_s(M_Z) \lesssim 0.123$. In this case they reproduce the exact results of the calculation with maximal errors of $\delta s^2_{eff} \sim 1\times 10^{-5}$, $\delta M_W \lesssim 1$ MeV and $\delta\Gamma_\ell \lesssim 3$ KeV, which are all very much below the experimental accuracy. Outside the above range, the deviations increase but remain very small for larger Higgs mass, reaching about 3×10^{-5}, 3 MeV, and 4 KeV at $M_H = 600$ GeV for $\sin^2\theta_{eff}^{lept}$, M_W, Γ_ℓ, respectively.

By comparing the normalized coefficients of $\ln M_H$ in Eqs. (21) and (22), we see that $\sin^2\theta_{eff}^{lept}$ is ~ 3 times more sensitive to $\ln M_H$ than M_W, ~ 6.6 times more sensitive to $\Delta\alpha_h$, almost 2 times more sensitive to M_t and α_s. Concerning Γ_ℓ, table 5 shows a sensitivity to $\ln M_H$ comparable to that of M_W. Its present experimental determination, however, is less

Scheme	Γ_ℓ^0	$10^2 g_1$	$10 g_2$	$10 g_3$	$10 g_4$	$10^2 g_5$
$\overline{\mathrm{MS}}$	84.0112	5.37	4.76	8.01	1.13	2.14
OSI	84.0122	5.39	4.76	8.02	1.12	2.16
OSII	84.0099	5.49	4.75	7.99	1.12	2.16

Table 5: Values of Γ_ℓ^0 and g_i in Eq. (23), in MeV, as in Table 3.

precise and it is not expected to improve significantly in the foreseeable future. Despite the recent progresses in the measurement of M_W, it is clear that most of the present sensitivity to M_H still comes from the effective sine. However, with an improvement in the measurements of both M_W and M_t the situation may change in the future [7–9].

We now use Eqs.(21–23) together with the latest data to determine M_H by a χ^2 analysis. The experimental inputs we use are [42]: $\sin^2\theta_{eff}^{lept} = 0.23157 \pm 0.00018$, $M_W = 80.394 \pm 0.042$ GeV, $\Gamma_\ell = 83.90 \pm 0.10$ MeV, $M_t = 174.3 \pm 5.1$GeV, $\alpha_s(M_Z) = 0.119 \pm 0.003$. Concerning $(\Delta\alpha)_h$ we adopt the value 0.02804 ± 0.00065 [43] but will comment later on the impact of some recent estimates [44]. The dependence on the scheme of our result is very mild. The $\overline{\mathrm{MS}}$ scheme leads to the highest M_H value. The $\ln(M_H/100)$ is to good approximation normally distributed and we obtain in $\overline{\mathrm{MS}}$ scheme $\ln M_H/100 = -0.04 \pm 0.64$, corresponding to a central value $M_H = 96$ GeV and to a 95% probability upper limit of about 270 GeV. Repeating the same analysis in the other two schemes, we obtain 95% upper limits that differ from the one in $\overline{\mathrm{MS}}$ by at most -15 GeV. One should also consider the uncertainty due to uncalculated QCD corrections. The dominant QCD effect is linked to the leading $O(G_\mu M_t^2)$ contribution to $\Delta\rho$, and in particular to the top quark mass definition. A simple way to take the related uncertainty into account is through a systematic shift of M_t. Indeed, the conservative values for the QCD uncertainty given in [7, 8] correspond to a variation of $\delta M_t = \pm 0.9$ GeV. An increase of 0.9 GeV in the central value of the top mass moves the M_H 95% upper bound by about +15 GeV. Thus $M_H \lesssim 285$ GeV could be taken as a 95% probability upper limit obtained using only indirect information and including the theory uncertainty. Finally, we note that a corresponding analysis carried out without implementing the $O(g^4 M_t^2/M_W^2)$ corrections gives a central value and upper bound for M_H significantly larger, by about 40 and 90 GeV, respectively.

Following Ref. [10], we can include in the M_H analysis the information coming from the direct search experiments presently in operation at LEP. The combination of the search data, for center of mass energy up to $\sqrt{s} = 183$ GeV, with the above result from precision measurements moves the central value for M_H from 96 to 145 GeV, while the 95% probability upper limit including the theory uncertainty reaches 345 GeV. The uncertainty on the upper bound due to the simplified likelihood procedure adopted has been estimated in [10] to be $O(5\,\mathrm{GeV})$.

Because of the strong correlation between M_t and M_H, apparent in Eqs.(21-23), in a

global fit also observables insensitive to the Higgs boson can have an indirect effect in the M_H determination. In particular, the prediction for R_b is almost independent of M_H, but the present experimental value $R_b = 0.21680 \pm 0.00073$ points towards a much lighter top ($M_t \approx 140 \pm 24$ GeV) than most other data. A smaller M_t central value favors a lighter M_H and consequently leads to a reduced 95% upper bound. The inclusion of R_b in the fit, for example, would lower the M_H central value and upper limit by approximately 10 and 30 GeV, respectively. Our analysis, in any case, is based only on M_W, $\sin^2\theta_{eff}^{lept}$, and Γ_ℓ, the three best measured observables which are also known to $O(g^4 M_t^2/M_W^2)$.

Several new estimates of the hadronic contribution to the running of α have appeared over the last couple of years [44]. These new investigations differ from the previous most phenomelogical analyses [43] mainly by the use of perturbative QCD (pQCD) down to energies of the order of a few GeV and by the treatment of old experimental data in regions where pQCD is not applicable. The combination of these two factors gives a result for $(\Delta\alpha)_h$ with a drastically reduced uncertainty but, at the same time, with a lower central value. Since these new estimates remove a significant part of the theoretical error in the prediction of $\sin^2\theta_{eff}^{lept}$, they further enhance its role in the indirect M_H determination. As can be seen from the sign of the coefficient c_2 in Eq. (21), a smaller central value for $(\Delta\alpha)_h$ prefers a heavier Higgs. There is therefore a compensation between the reduced error and the lower central value so that only the very high confidence level values are significantly reduced. As an illustration, we perform the M_H analysis using the $\Delta\alpha_h$ determination with the smallest error, due to Davier and Hocker, i.e. $\Delta\alpha_h = 0.02770 \pm 0.00016$. The $\overline{\mathrm{MS}}$ fit, without including theoretical errors and the information from direct searches, has a central value at $M_H = 122$ GeV and an upper bound only 10 GeV smaller than the one obtained with the $\Delta\alpha_h$ determination of [43].

6 Summary

The $O(g^4 M_t^2/M_W^2)$ corrections have been calculated for many accurately measured precision observables and are now implemented in several global fit programs [45–47]. The only important quantities whose predictions are not known at the same order are those connected with b-final states because their $O(g^4 M_t^2/M_W^2)$ contributions involve specific two-loop vertex corrections.

In this paper we have presented the results of the calculation of the partial widths Γ_f ($f \neq b$) of the Z^0 boson to $O(g^4 M_t^2/M_W^2)$ in three different electroweak renormalization schemes. In the case of Γ_ℓ, the size of these contributions is modest (up to 34 KeV) when compared to the present experimental error (90 KeV), but, like for M_W and the effective sine, their inclusion sharply reduces the scheme dependence of the theoretical predictions. The situation is very similar for the partial widths into quarks. Concerning Γ_u and Γ_d, in the case of a light Higgs of 100 GeV the $O(g^4 M_t^2/M_W^2)$ corrections induce the variations $\Delta\Gamma_u = -63$ KeV and $\Delta\Gamma_d = -85$ KeV in the $\overline{\mathrm{MS}}$ scheme, $\Delta\Gamma_u = -62$ KeV and $\Delta\Gamma_d = -73$ KeV in OSI, while the shifts in OSII are approximately twice larger, $\Delta\Gamma_u \simeq \Delta\Gamma_d = -175$ KeV. It is interesting to compare these shifts with the ones

due to non-factorizable $O(\alpha\alpha_s)$ corrections to the hadronic width: $\Delta\Gamma_u = -124$ KeV, $\Delta\Gamma_d = -173$ KeV [50]. Adding the contributions of the u, d, s, c quarks, the overall shift to the total hadronic width Γ_h may reach 0.7 MeV, to be compared to the present experimental error of 2.3 MeV.

We have also described in detail several aspects of the $O(g^4 M_t^2/M_W^2)$ calculations, which had not been reported in previous publications. Furthermore, in appendix A we have presented explicit expressions for the two-loop $O(g^4 M_t^2/M_W^2)$ contribution to the self-energies of the W and Z^0 bosons.

The analytic results of the calculations for M_W, $\sin^2\theta_{eff}^{lept}$, and Γ_ℓ, together with the relevant QCD corrections, have been incorporated in a numerical code, from which we have derived simple interpolating formulae following Ref. [7]. They reproduce very accurately the results of the code for a large range of values of the input parameters. At present, one of the most interesting application of high precision investigations is the attempt to constrain the Higgs boson mass from the data. As has been repeatedly observed [4, 7–9], our $O(g^4 M_t^2/M_W^2)$ calculations do have a significant impact on the Higgs mass bound, because of an enhancement of the *screening* operated by the higher order contributions on the leading one-loop correction. Using the interpolating formulae, it is very simple to obtain an indirect determination of M_H based on the latest preliminary data. The result of our analysis using only the indirect information from precision measurements gives $M_H < 285$ at 95% C.L., where the theoretical uncertainty is also taken into account. The inclusion of the direct search information up to energies $\sqrt{s} = 183$ GeV according to the procedure outlined in [10] increases the 95% upper limit by ~ 60 GeV. As a final remark, we notice that the Higgs determination is very sensitive to the value of the effective sine employed in the analysis and that the above results have been obtained using the SLD+LEP average. Although recently the discrepancy between the LEP and SLD $\sin^2\theta_{eff}^{lept}$ determinations has somewhat receded, it should be kept in mind that their agreement is still far from satisfactory.

Acknowledgements

We are grateful to S. Fanchiotti, F. Feruglio, M. Passera, A. Sirlin, and A. Vicini for collaboration on different projects variously connected to the subject of this paper. We also thank P.A. Grassi, G. Passarino, and M. Steinhauser for interesting communications and discussions. This work has been supported in part by the Bundesministerium für Bildung und Forschung under contract 06 TM 874 and by the DFG project Li 519/2-2.

Appendix A

In this appendix we present some of the intermediate results. The analytic expressions for the irreducible two-point functions of the W and the Z^0 bosons through $O(g^4 M_t^2/M_W^2)$ are extremely long and cannot be reduced to a compact form. However, after on-shell

renormalization of the masses inside the loops, i.e. after adding the mass counterterm diagrams, they simplify considerably.

The expressions for the two-loop self-energies that follow are calculated in the 't Hooft-Feynman gauge and include all the irreducible unrenormalized diagrams that contribute to the order of the calculation plus the corresponding contributions from the on-shell mass counterterms of the particles in the loops. Neither gauge coupling nor wave-function renormalization are carried out. The renormalization of the unphysical Z^0 and W sectors is performed according to the *heavy mass* procedure described in Sec. 2, so that all two-loop vertex and box contributions proportional to powers of M_t are canceled, and only two-loop self-energies have to be taken into account.

As the couplings of the SM sometimes contain masses, which we renormalize in the same way as the ones that appear in the propagators, a possible ambiguity arises in the $\overline{\rm MS}$ scheme, because it is always possible to rewrite M_W as $M_Z\hat{c}$ in the couplings of a one-loop diagram; the counterterm associated to the two forms differ in the finite part. In order to avoid any possible source of confusion, it is important to stress here that all our two-loop expressions are therefore consistent only with the choices adopted in the one-loop $\overline{\rm MS}$ expressions reported in [5,32]. Different choices would induce different $O(g^4 M_t^2/M_W^2)$ terms.

We first introduce some functions which appear in the following expressions of $A_{WW}(q^2)$ and $A_{ZZ}(q^2)$ and in the formulae of the next appendix. We define:

$$g(x) = \begin{cases} \sqrt{4-x}\,\left(\pi - 2\arcsin\sqrt{x/4}\right) & 0 < x \le 4 \\ \\ 2\sqrt{x/4-1}\,\ln\left(\frac{1-\sqrt{1-4/x}}{1+\sqrt{1-4/x}}\right) & x > 4\ , \end{cases}$$

$$\Lambda(x) = \begin{cases} -\frac{1}{2\sqrt{x}}\,g(x) + \frac{\pi}{2}\sqrt{4/x-1} & 0 < x \le 4 \\ \\ -\frac{1}{2\sqrt{x}}\,g(x) & x > 4\ , \end{cases}$$

where we have indicated the dilogarithmic function as ${\rm Li}_2(x) = -\int_0^x dt\,\frac{\ln(1-t)}{t}$, and we introduce

$$\phi(z) = \begin{cases} 4\sqrt{\frac{z}{1-z}}\; Cl_2(2\arcsin\sqrt{z}) & 0 < z \le 1 \\ \frac{1}{\lambda}\left[-4{\rm Li}_2(\frac{1-\lambda}{2}) + 2\ln^2(\frac{1-\lambda}{2}) - \ln^2(4z) + \pi^2/3\right] & z > 1\,, \end{cases}$$

where $Cl_2(x) = {\rm Im}\,{\rm Li}_2(e^{ix})$ is the Clausen function and $\lambda = \sqrt{1-\frac{1}{z}}$.

The function $B_0[q^2, m_1^2, m_2^2]$ is defined through the one-loop integral ($\epsilon = (4-n)/2$)

$$-\,i\,M_t^{2\epsilon} e^{\gamma\epsilon} \int \frac{d^n k}{\pi^{n/2}} \frac{1}{[k^2 - m_1^2][(k-q)^2 - m_2^2]} = \frac{1}{\epsilon} + B_0[q^2, m_1^2, m_2^2] + O(\epsilon), \qquad \text{(A1)}$$

whose analytic form is well known (see for example Ref. [48]). It is interesting to note that the $O(\epsilon)$ part of one-loop integrals like the one in Eqs. (A1) cancel exactly in the two-loop expressions of the self-energies given below.

We also introduce the following short-hand notation:

$$\boxed{\begin{array}{cccc} w = M_W^2; & z = M_Z^2; & h = M_H^2; & t = M_t^2; \\ w_t = \frac{w}{t}; & z_t = \frac{z}{t}; & h_t = \frac{h}{t}. & \end{array}}$$

As no coupling renormalization has been carried out in the following self-energies, we express the results in terms of unspecified sine and cosine s, c of the Weinberg angle which should *not* be understood as *on-shell* quantities.

- $A_{ZZ}(q^2)$

In order to fix completely the one-loop contribution we report here the coefficient of the $1/\epsilon$ pole term that is not explicitly written in Ref. [5]

$$A_{ZZ}^{(1)\,pole} = \frac{g^2}{(16\pi^2)} \left[q^2 \left(\frac{41}{3} - \frac{41}{6\,c^2} - \frac{23\,c^2}{3} \right) + \frac{3}{2\,c^2} M_t^2 + \left(4 - \frac{2}{c^2} \right) M_W^2 - \frac{M_Z^2}{c^2} \right] \tag{A2}$$

where M_t, M_W and M_Z are understood as OS masses. Concerning the HTE of the two-loop self-energy, as explained in Sec. 3, we have to distinguish between the case in which the Higgs is light relative to the top quark, and the one in which it is comparable to it. In the first case, the result, expressed in units $N_c g^4/c^2\ M_t^2/(16\pi^2)^2\ (\mu/M_t)^{4\epsilon}$ $(N_c = 3)$, reads

$$\begin{aligned}
A_{ZZ}^{(2)}(q^2) = & \left(\frac{13}{24} + \frac{1}{48\,c^2} + \frac{3}{16\,w_t} \right) \frac{1}{\epsilon^2} \\
& + \left[\sqrt{h_t}\,\pi \frac{3\,h_t - 8}{16\,w_t} - \frac{1}{8\,c^2} \ln z_t - \frac{1}{4} \ln w_t + \left(\frac{17}{72} - \frac{17c^2}{36} + \frac{13c^4}{36} \right) \frac{q^2}{w} - c^2 \right. \\
& \left. + \frac{197}{144} + \frac{29}{288c^2} + \frac{3h}{8\,w} + \frac{23}{32\,w_t} - \frac{3\,h}{8\,w} \ln h_t \right] \frac{1}{\epsilon} + \frac{h\,\left(c^2\,\left(2\,h + 5\,q^2\right) - 2\,w\right)}{36\,c^2\,q^2\,w} \ln h_t \\
& + \left(\frac{1}{12} + \frac{1}{48\,c^2} - \frac{1}{48\,w_t} \right) \pi^2 - \frac{81h + 136q^2 - 320c^2q^2 + 256c^4q^2 - 216t}{432\,w} \sqrt{h_t}\,\pi \\
& + \frac{c^2(h - q^2) - w}{18\,c^4\,q^2} \ln c^2 + \left(\frac{1}{18\,c^2} - \frac{1}{24} + \frac{c^2}{3} - \frac{h}{18c^2q^2} + \frac{w}{18\,c^4\,q^2} \right) \ln w_t \\
& + \left(\frac{5}{6} - \frac{2\,c^2}{3} + \frac{q^2}{24w} - \frac{c^2\,q^2}{12w} \right) B_0[q^2, w, w] - \frac{q^2}{18w}(1 + 2c^2) \ln \left(\frac{-q^2}{M_t^2} \right) - \frac{1}{2} \delta_t \\
& + \left(\frac{5q^2 - h}{9\,c^2} + \frac{(h - q^2)^2}{18\,w} + \frac{w}{18c^4} \right) \frac{B_0[q^2, h, z]}{q^2} + \left(\frac{61}{108} - \frac{191c^2}{216} + \frac{61c^4}{72} \right) \frac{q^2}{w} \\
& - \frac{(h - z)^2}{18\,w\,q^2} - \frac{17}{96} + \frac{55}{192c^2} - \frac{c^2}{2} - \frac{7h}{48w} - \frac{45}{64w_t}.
\end{aligned} \tag{A3}$$

Here and henceforth δ_t is the $O(\epsilon)$ part of the top mass counterterm calculated at $\mu = M_t$ which cancels out in the physical amplitudes we have considered. In the case of a heavy Higgs boson, the HTE takes the form, in the same units:

$$
\begin{aligned}
A^{(2)}_{ZZ}(q^2) = & \left(\frac{13}{24} + \frac{1}{48\,c^2} + \frac{3}{16\,w_t}\right)\frac{1}{\epsilon^2} \\
& + \left[\frac{h_t - 4}{16\,w_t} g(h_t)\sqrt{h_t} - \frac{\ln z_t}{8\,c^2} - \frac{\ln w_t}{4} + \left(\frac{17}{72} - \frac{17c^2}{36} + \frac{13c^4}{36}\right)\frac{q^2}{w} - c^2 + \frac{197}{144}\right. \\
& \left. + \frac{29}{288c^2} - \frac{h}{8\,w} + \frac{23}{32\,w_t} + \frac{h_t(h_t-6)}{16\,w_t}\ln h_t\right]\frac{1}{\epsilon} - \frac{q^2}{18w}(1+2c^2)\ln\left(\frac{-q^2}{M_t^2}\right) \\
& + \left(\frac{1}{12} + \frac{1}{48\,c^2} - \frac{1}{48\,w_t}\right)\pi^2 + \left(\frac{5}{6} - \frac{2\,c^2}{3} + \frac{q^2}{24w} - \frac{c^2\,q^2}{12w}\right) B_0[q^2, w, w] - \frac{1}{2}\delta_t \\
& + \left[\frac{3(h_t-4)}{8c^2\,h_t} + \frac{h(7-h_t)}{16\,w} + \frac{q^2}{w}\left(\frac{(4c^2-5)c^2(6+27h_t-10{h_t}^2+{h_t}^3)}{54\,(h_t-4)}\right.\right. \\
& \left.\left. - \frac{1152 + 606h_t + 1467{h_t}^2 - 1097{h_t}^3 + 238{h_t}^4 - 17{h_t}^5}{432(h_t-4)^2\,h_t}\right)\right]\ln h_t \\
& + \left(\frac{h_t}{4} - 1\right)\left[\frac{q^2}{w}\left(\frac{17}{108} - \frac{10\,c^2}{27} + \frac{8\,c^4}{27}\right) - \frac{1}{4\,w_t}\right]\sqrt{h_t}\,g(h_t) - \frac{17}{96} + \frac{7}{192\,c^2} \\
& - \frac{c^2}{2} + \frac{h}{16w} - \frac{77}{64w_t} + \left(\frac{c^2}{3} - \frac{1}{24}\right)\ln w_t + \left[\frac{3\,(4-h_t)\,(h_t-2)}{16c^2\,{h_t}^2} + \frac{3}{16\,w_t}\right. \\
& \left. + \frac{q^2}{w}\left(\frac{c^2\,(5-4\,c^2)\,(h_t-1)}{9\;(h_t-4)\;h_t} - \frac{384 + 10h_t - 238\,h_t^2 + 63\,h_t^3 - 3\,h_t^4}{144\,(h_t-4)^2\,{h_t}^2}\right)\right]\phi(\frac{h_t}{4}) \\
& + \left(\frac{3}{c^2\,h_t} - \frac{3}{4\,c^2} - \frac{h}{8\,w} - \frac{q^2}{12\,w} + \frac{1}{2\,w_t} + \frac{q^2}{3\,h_t\,w}\right)\Lambda(h_t) \\
& + \frac{q^2}{w}\left[\frac{(-17+40\,c^2-32\,c^4)\,h_t}{216} + \frac{5}{144\,(h_t-4)} + \frac{791}{864} - \frac{251\,c^2}{216} + \frac{77\,c^4}{72}\right].
\end{aligned}
\tag{A4}
$$

- $A_{WW}(q^2)$

The coefficient of one-loop pole is

$$
A^{(1)\,pole}_{WW} = \frac{g^2}{(16\pi^2)}\left[-\frac{5}{6}q^2 + \frac{3}{2}M_t^2 - \frac{s^2}{c^2}M_W^2 + M_Z^2\,c^2\right] \quad . \tag{A5}
$$

In the case of a light Higgs, the HTE for the two-loop W self-energy takes the form, in units $N_c g^4\,M_t^2/(16\pi^2)^2\;(\mu/M_t)^{4\epsilon}$,

$$
\begin{aligned}
A^{(2)}_{WW}(q^2) = & \left(\frac{13}{24} + \frac{1}{48\,c^2} + \frac{3}{16\,w_t}\right)\frac{1}{\epsilon^2} \\
& + \left[\sqrt{h_t}\,\pi\frac{3\,h_t - 8}{16\,w_t} - \frac{1}{8\,c^2}\ln z_t - \frac{1}{4}\ln w_t + \frac{q^2}{8w} + \frac{233}{144} + \frac{101}{288c^2}\right. \\
& \left. + \frac{3h}{8\,w} + \frac{23}{32\,w_t} - \frac{3\,h}{8\,w}\ln h_t\right]\frac{1}{\epsilon} + \frac{h\;(5\,h - q^2 - 5\,w)}{144\,q^2\,w}\ln h_t - \frac{1}{2}\delta_t
\end{aligned}
$$

$$
\begin{aligned}
&+\left(\frac{23}{108}-\frac{55}{216\,c^2}+\frac{h}{8\,w}-\frac{q^2}{36\,w}-\frac{7}{48\,w_t}\right)\pi^2-\frac{c^2\,q^2+s^2w}{48\,c^4\,q^2}\ln c^2\\
&+\left(\frac{3w-5\,c^4\,h+3c^2\,q^2-46c^4q^2-6\,c^2\,w+8\,c^4\,w}{144\,c^4\,q^2}\right)\ln w_t\\
&+\left(\frac{11-13\,c^2}{24\,c^2}+\frac{q^2}{48\,w}+\frac{s^4\,w}{48\,c^4\,q^2}\right)B_0[q^2,w,z]+\frac{31q^2}{48w}\\
&+\left(5\,q^2-h+\frac{(h-q^2)^2}{2\,w}+\frac{w}{2}\right)\frac{5\,B_0[q^2,h,w]}{72q^2}+\frac{24t-9\,h-32\,q^2}{96\,w}\sqrt{h_t}\,\pi\\
&+\left(\frac{10h}{w}-8-\frac{3}{c^4}+\frac{6}{c^2}-\frac{5h^2}{w^2}\right)\frac{w}{144q^2}-\frac{155}{288}+\frac{1633}{576c^2}-\frac{29h}{24w}+\frac{31}{64w_t},
\end{aligned}
\tag{A6}
$$

while in the case of a heavy Higgs, we find in the same units:

$$
\begin{aligned}
A^{(2)}_{WW}(q^2)=&\left(\frac{13}{24}+\frac{1}{48\,c^2}+\frac{3}{16\,w_t}\right)\frac{1}{\epsilon^2}\\
&+\Bigg[\sqrt{h_t}\,g(h_t)\frac{h_t-4}{16\,w_t}-\frac{1}{8\,c^2}\ln z_t-\frac{1}{4}\ln w_t+\frac{q^2}{8w}+\frac{233}{144}+\frac{101}{288c^2}\\
&-\frac{h}{8\,w}+\frac{23}{32\,w_t}+\frac{h_t\,(h_t-6)}{16\,w_t}\ln h_t\Bigg]\frac{1}{\epsilon}+\frac{(4-h_t)\,(3\,h+2\,q^2+18\,w)}{24\,h\,w_t}\Lambda(h_t)\\
&+\left(\frac{23}{108}-\frac{55}{216\,c^2}+\frac{1}{16\,h_t}-\frac{1}{24\,h_t^2}+\frac{1}{96\,w_t}-\frac{7\,q^2}{144\,h_t\,w}-\frac{1}{16\,h_t\,w_t}-\frac{19\,q^2}{432\,h_t^2\,w}\right)\pi^2\\
&+\left(\frac{11-13c^2}{24\,c^2}+\frac{q^2}{48\,w}+\frac{s^4\,w}{48c^4\,q^2}\right)B_0[q^2,w,z]-\frac{c^2\,q^2+s^2w}{48\,c^4\,q^2}\ln c^2\\
&+\left[\frac{5}{16}-\frac{7}{4\,h_t}-\frac{3}{8\,w_t}+\frac{h_t}{16\,w_t}-\frac{{h_t}^2}{32\,w_t}+\frac{q^2}{w}\left(\frac{1}{36}-\frac{31}{72\,h_t}-\frac{h_t}{8}+\frac{{h_t}^2}{24}\right)\right]\ln h_t\\
&+\sqrt{h_t}\,g(h_t)\,(h_t-4)\,\frac{4\,q^2-3\,t}{96\,w}+\left(\frac{1-17\,c^2}{48\,c^2}+\frac{s^4\,w}{48\,c^4\,q^2}\right)\ln w_t-\frac{s^4\,w}{48\,c^4\,q^2}\\
&+\frac{h_t-4}{288{h_t}^2\,w}\Big(12q^2-34\,h_t\,q^2-26\,{h_t}^2\,q^2+18{h_t}^3\,q^2+54\,{h_t}^2\,t-27{h_t}^3\,t+108\,w\\
&-18\,h_t\,w+18{h_t}^2\,w\Big)\,\phi\Big(\frac{h_t}{4}\Big)+\Big(38q^2+42\,h_t\,q^2-24\,{h_t}^2\,q^2-62{h_t}^3\,q^2+18{h_t}^4\,q^2\\
&+54h_t\,t-135\,{h_t}^2\,t+108\,{h_t}^3\,t-27h_t^4t+36w-54h_t\,w+18h_t^3\,w\Big)\,\frac{\mathrm{Li}_2(1-h_t)}{144\,{h_t}^2\,w}\\
&-\frac{23}{72}+\frac{1633}{576\,c^2}+\frac{1}{4h_t}-\frac{3\,h}{16\,w}+\frac{23}{64\,w_t}+\frac{q^2}{w}\left(\frac{5}{36}+\frac{h_t}{24}+\frac{19}{72h_t}\right)-\frac{1}{2}\delta_t.
\end{aligned}
\tag{A7}
$$

The other self-energies used in the various $O(g^4M_t^2/M_W^2)$ calculations are the photon two-point function at $q^2=0$ and the $\gamma-Z^0$ mixing amplitude at $q^2=M_Z^2$. They are the only contributions to $\delta^{(2)}e/e|_{\overline{\rm MS}}$ and $\Delta\hat{k}^{(2)}$, respectively, and therefore can be read directly from Eqs. (B5) and (B3).

The limit for $q^2\to 0$ of the previous expressions can be easily obtained using the

expansion of $B_0[q^2,a,b]$ in powers of q^2:

$$B_0[q^2,a,b] = 1 - \frac{a\,\ln a - b\,\ln b}{a-b} + q^2 \frac{\left(a^2 - b^2 - 2\,a\,b\,\ln\frac{a}{b}\right)}{2\,(a-b)^3} + O(q^4) \tag{A8}$$

As an example of the use of the above self-energies, we now calculate the $\overline{\rm MS}$ counterterm $\delta\hat{s}^2$ at $O(g^4 M_t^2/M_W^2)$. We recall that, following Eq. (12b) of Ref. [5], $\delta\hat{s}^2 = -M_W^2/M_Z^2\, Y|_{pole}$, where Y is the expression appearing on the r.h.s of Eq. (13), before the poles are subtracted. Inserting the poles of Eqs. (A3) and (A6) or Eqs. (A4) and (A7) into the previous relation is not sufficient to obtain the correct result in the pure $\overline{\rm MS}$ scheme because (i) no one-loop coupling renormalization has yet been carried out and (ii) the two-loop self-energies have been obtained using OS masses instead of a pure $\overline{\rm MS}$ subtraction. The $\overline{\rm MS}$ renormalization of gauge couplings does not introduce M_t^2 terms and at $O(g^4 M_t^2/M_W^2)$ it is only needed for the leading quadratic contribution. Working as usual in n dimensions, we find

$$-\frac{\delta\hat{g}^2}{\hat{g}^2} Y_{\overline{\rm MS}}^{(1,lead)} = -\frac{19}{6}\frac{N_c\,\hat{g}^4}{(16\pi^2)^2}\frac{M_t^2}{4M_W^2}\left(\frac{1}{\epsilon} + \frac{1}{2} - \ln\frac{M_t^2}{\mu^2} + O(\epsilon)\right). \tag{A9}$$

In order to re-express the poles of the two-loop self-energies in terms of $\overline{\rm MS}$ quantities we take Eqs. (A2) and (A5), insert them in $M_W^2/M_Z^2\, Y$, replace M_W^2/M_Z^2 by $\hat{c}^2(1 + \frac{\hat{c}^2}{\hat{s}^2}\Delta\hat{\rho}^{(1)}_{lead})$ in n dimensions, and expand at $O(g^4 M_t^2/M_W^2)$. The extra term at this order reads

$$Y^{(2)}_{extra} = -\frac{N_c\,\hat{g}^4}{(16\pi^2)^2}\frac{M_t^2}{4M_W^2}\left(\frac{1}{\epsilon} + \frac{1}{2} - \ln\frac{M_t^2}{\mu^2} + O(\epsilon)\right)\left(4\hat{c}^2 - \frac{13}{6} + \frac{1}{\hat{c}^2}\right). \tag{A10}$$

Combining the poles of the two-loop self-energies in Y together with Eqs. (A9) and $Y^{(2)}_{extra}$, we find the correct $\overline{\rm MS}$ counterterm

$$\frac{\delta^{(2)}\hat{s}^2}{\hat{s}^2} = -\frac{N_c\,\hat{g}^4}{(16\pi^2)^2}\,\frac{M_t^2}{\hat{c}^2 M_Z^2}\,\frac{1}{\epsilon}\left(\frac{1}{8} - \frac{13}{36}\,\hat{s}^2\right), \tag{A11}$$

which can be checked with [49]. Combining the finite parts of these three components, instead, one obtains $\Delta\hat{\rho}^{(2)}$ given in [3].

Appendix B

In this Appendix we present the two-loop $O(g^4 M_t^2/M_W^2)$ contributions to the electroweak corrections entering the Z decay partial widths.

We begin by considering the $\hat{\eta}$ and $\hat{k}$ corrections of the $\overline{\rm MS}$ framework. We have for $M_H \ll M_t$ in units $N_c/(16\pi^2)\,(\hat{\alpha}/4\pi\hat{s}^2)\,M_t^2/(M_Z^2\hat{c}^2)$

$$\Delta\hat{\eta}^{(2)} = \frac{h_t^3 - 6\,h_t^2\,z_t + 11\,h_t\,{z_t}^2}{9\,\hat{c}^2\,(h_t - 4\,z_t)\,z_t^2} + \frac{49 - 289\,\hat{c}^2 - 349\,\hat{c}^4 + 292\,\hat{c}^6}{216\,\hat{c}^2\,(1 - 4\,\hat{c}^2)}$$

$$
\begin{aligned}
&+ \frac{1+18\,\hat{c}^2-16\,\hat{c}^4}{12\,(1-4\,\hat{c}^2)}\ln\hat{c}^2 - \frac{17-40\,\hat{c}^2+32\,\hat{c}^4}{54\,\hat{c}^2}(\sqrt{h_t}\,\pi-2) \\
&+ \frac{11\,h_t^2\,z_t - 2\,h_t^3 - 24\,h_t\,z_t^2 + 24\,z_t^3}{18\,\hat{c}^2\,(h_t-4\,z_t)\,z_t^2}\ln h_t + \frac{1-4\,\hat{c}^2+44\,\hat{c}^4-32\,\hat{c}^6}{24\,\hat{c}^2(1-4\,c^2)}B_0[z,w,w] \\
&+ \frac{13\,h_t^2\,z_t - 2\,h_t^3 - 32\,h_t\,z_t^2 + 36\,z_t^3}{18\,\hat{c}^2\,(h_t-4\,z_t)\,{z_t}^2}B_0[z,h,z] - \frac{17-34\,\hat{c}^2+26\,\hat{c}^4}{36\,\hat{c}^2}\ln\frac{M_t^2}{\mu^2} \\
&+ \left(\frac{h_t\,(2h_t-5z_t)}{18\,\hat{c}^2\,z_t\,(h_t-4\,z_t)} + \frac{10-39\,\hat{c}^2-70\,\hat{c}^4+48\,\hat{c}^6}{36\,\hat{c}^2\,(4\,\hat{c}^2-1)}\right)\ln z_t. \qquad \text{(B1)}
\end{aligned}
$$

In the case of $M_H \gg M_Z$ we obtain in the same units

$$
\begin{aligned}
\Delta\hat{\eta}^{(2)} = {} & \frac{(-17+40\,\hat{c}^2-32\,\hat{c}^4)\,h_t}{216\,\hat{c}^2} + \frac{5}{144\,\hat{c}^2\,(h_t-4)} + \frac{707-4720\,\hat{c}^2+5900\,\hat{c}^4-3696\,\hat{c}^6}{864\,\hat{c}^2\,(1-4\,\hat{c}^2)} \\
&+ \left(\frac{10}{27} - \frac{17}{108\,\hat{c}^2} - \frac{8\,\hat{c}^2}{27}\right)(1-\frac{h_t}{4})\sqrt{h_t}\,g(h_t) + \frac{1+18\hat{c}^2-16\hat{c}^4}{12\,(1-4\,\hat{c}^2)}\ln\hat{c}^2 + \frac{4-h_t}{12\,\hat{c}^2\,h_t}\Lambda(h_t) \\
&+ \frac{2-7\,\hat{c}^2-70\,\hat{c}^4+48\,\hat{c}^6}{36\,\hat{c}^2\,(4\,\hat{c}^2-1)}\ln z_t + \frac{1-4\,\hat{c}^2+44\,\hat{c}^4-32\,\hat{c}^6}{24\,\hat{c}^2\,(1-4\,\hat{c}^2)}B_0[z,w,w] \\
&- \frac{17-34\hat{c}^2+26\hat{c}^4}{36\,\hat{c}^2}\ln\frac{M_t^2}{\mu^2} + \left[\frac{(4\hat{c}^2-5)\,(6+27h_t-10h_t^2+h_t^3)}{54\,(h_t-4)}\right. \\
&- \left.\frac{1152+606h_t+1467{h_t}^2-1097{h_t}^3+238{h_t}^4-17{h_t}^5}{432\,\hat{c}^2(h_t-4)^2\,h_t}\right]\ln h_t \\
&+ \left[\frac{(5-4\,\hat{c}^2)\,(h_t-1)}{9\,(h_t-4)\,h_t} - \frac{384+10\,h_t-238\,{h_t}^2+63\,{h_t}^3-3\,{h_t}^4}{144\,\hat{c}^2\,(h_t-4)^2\,{h_t}^2}\right]\phi(\frac{h_t}{4}). \qquad \text{(B2)}
\end{aligned}
$$

The correction $\hat{k}$ can be written as $\hat{k}_f = 1 + (\hat{e}^2/\hat{s}^2)(\Delta\hat{k}_f^{(1)} + \Delta\hat{k}_f^{(2)})$ where the two-loop part has been given already in Ref. [4]. We report here again for completeness. Considering $M_H \gg M_t$ in units $N_c/(16\pi^2)(\hat{\alpha}/(4\pi\hat{s}^2))M_t^2/(c^2M_Z^2)$ one has

$$
\begin{aligned}
\mathrm{Re}\,\Delta\hat{k}^{(2)}(M_Z^2) = {} & \frac{-211+24\,h_t+462\,\hat{s}^2-64\,h_t\,\hat{s}^2}{432} + \left(\frac{3}{8}-\frac{\hat{s}^2}{3}\right)B_0[z,w,w] - \frac{\hat{c}^2}{6}\ln\hat{c}^2 \\
&+ \frac{(h_t-4)\,\sqrt{h_t}\,(8\,\hat{s}^2-3)\,g(h_t)}{108} - \frac{\left(6+27\,h_t-10\,{h_t}^2+{h_t}^3\right)\,(3-8\,\hat{s}^2)}{108\,(h_t-4)}\ln h_t \\
&- \left(\frac{1}{4}+\frac{2}{9}\hat{s}^2\right)\ln\frac{M_t^2}{\mu^2} + \frac{(3\,\hat{s}^2-2)}{18}\ln z_t + \frac{(h_t-1)\,(8\,\hat{s}^2-3)}{18\,(4-h_t)\,h_t}\phi(\frac{h_t}{4}). \qquad \text{(B3)}
\end{aligned}
$$

In the case of a light Higgs mass, this becomes

$$
\begin{aligned}
\mathrm{Re}\,\Delta\hat{k}^{(2)}(M_Z^2) = {} & \frac{-175+366\,\hat{s}^2}{432} + \left(\frac{3}{8}-\frac{\hat{s}^2}{3}\right)B_0[z,w,w] - \frac{\hat{c}^2}{6}\ln\hat{c}^2 \\
&- \frac{2\pi}{27}\sqrt{h_t}\,(8\hat{s}^2-3) - \left(\frac{1}{4}+\frac{2}{9}\hat{s}^2\right)\ln\frac{M_t^2}{\mu^2} + \frac{(3\,\hat{s}^2-2)}{18}\ln z_t \qquad \text{(B4)}
\end{aligned}
$$

Numerically, $\mathrm{Re}\,\Delta\hat{k}^{(2)}(M_Z^2)$ is tiny, and the use of the expansion for light Higgs does not lead to any appreciable difference over the other one.

We give also the two-loop finite part of the electric charge counterterm, which is needed to calculate the $\overline{\rm MS}$ electromagnetic coupling. We have in units $N_c\,\hat\alpha^2/(16\pi^2 s^2) M_t^2/(M_Z^2\hat c^2)$

$$\left.\frac{2\delta^{(2)}e}{e}\right|_{\overline{\rm MS}} = \frac{231-32\,h_t}{216} - \frac{2}{27}(4-h_t)\sqrt{h_t}\,g(h_t) + \frac{2\left(6+27\,h_t-10\,{h_t}^2+{h_t}^3\right)}{27\,(h_t-4)}\ln h_t$$
$$- \frac{13}{18}\ln\frac{M_t^2}{\mu^2} - \frac{4\,(h_t-1)\,\phi(\frac{h_t}{4})}{9\,(h_t-4)\,h_t}, \tag{B5}$$

that in the case of a light Higgs reduces to $\frac{61}{72} - \frac{16\sqrt{h_t}\,\pi}{27} - \frac{13}{18}\ln\frac{M_t^2}{\mu^2}$.

We proceed to the discussion of the corrections of the OS scheme. Recalling Eq. (17) the additional two-loop contribution in $\Delta\bar\eta_f^{(2)}$ is given by (units $N_c x_t/(16\pi^2)$:

$$\Delta\bar\eta^{(2)}_{f,add} = 16\pi^2\Delta\bar\eta_f^{(1)} + V_{add} - \frac{197-1378\,c^2+1064\,c^4}{27\,(1-4\,c^2)}$$
$$-\frac{(1+16\,c^2-20\,c^4+48\,c^6)}{3(1-4c^2)}B_0[z,w,w] - \frac{2\,c^2\,(1+26\,c^2+24\,c^4)}{3(1-4c^2)}\ln c^2$$
$$+\left(\frac{41}{3}-\frac{46\,c^2}{3}\right)\ln\frac{M_t^2}{\mu^2} + \frac{2\,(50-283\,c^2+242\,c^4-72\,c^6)}{9(1-4c^2)}\ln z_t. \tag{B6}$$

where V_{add} contains the shifts of the one-loop vertices.

$$V_{add} = 8c^2\ln\frac{M_W^2}{\mu^2} + 3\left(I_f^3 Q_f - 4s^2Q_f^2\right)f_V(1) - 16c^2 g_V(c^{-2})$$
$$+\left(1-4c^2-2(1-2c^2)I_f^3Q_f\right)f_V(c^{-2}) \tag{B7}$$

and the functions $f_V(x)$ and $g_V(x)$ are defined in Eqs.(6d) and (6e) of [32].

The form factor k_f was considered in Ref. [4] only for the leptonic case. The generalization of Eq. (A4) of that reference to arbitrary fermions is (units $N_c x_t/(16\pi^2)$)

$$\Delta\bar k^{(2)}_{add,f} = \frac{-238\,c^2}{27} + 8c^4 - 2\,c^2\sqrt{4c^2-1}\left(3+4\,c^2\right)\arctan\!\left(\frac{1}{\sqrt{4\,c^2-1}}\right) - \frac{16}{9}c^2\ln z_t$$
$$+\frac{1-6\,I_f^3\,Q_f+8\,Q_f^2-8\,c^4\,Q_f^2}{4\,c^2}f_V(1) + 4\,c^2 g_V(c^{-2}) - 7\,c^2\,\ln c^2 - \frac{17}{3}c^2\ln\frac{\mu^2}{M_Z^2}$$
$$+c^2(1-Q_fI_f^3)f_V(c^{-2}) - \frac{80}{9}i\pi. \tag{B8}$$

To complete the discussion in the OS framework we need also the corrections $\Delta\bar\rho(s^2)$ and $\bar f(s^2)$. They have been considered in Ref. [4]. Recalling the definitions

$$\bar f(s^2) = \hat f^{(1)}(s^2) + \bar f^{(2)}(s^2) \tag{B9}$$
$$\Delta\bar\rho(s^2) = \Delta\hat\rho^{(1)}(s^2) + \Delta\bar\rho^{(2)}(s^2), \tag{B10}$$

where $\bar f^{(2)}(s^2) = \hat f^{(2)}(s^2) + \bar f^{(2)}_{add}(s^2)$, $\Delta\bar\rho^{(2)}(s^2) = \Delta\hat\rho^{(2)}(s^2) + \Delta\bar\rho^{(2)}_{add}(s^2)$, we have that $(G_\mu/\sqrt2)\,8M_W^2\,\Delta\hat\rho^{(2)}$ is given by Eqs.(10a,b) of Ref. [3] multiplied by $N_c x_t^2$ while $\Delta\bar\rho^{(2)}_{add}(s^2)$

is reported in Eq.(A2) of Ref. [4]. The amplitude $(e^2/s^2)\hat{f}^{(2)}$ is given by the sum of $(2\delta^{(2)}e/e)$ given in Eq. (B5) and Eqs.(7a,b)[5] of Ref. [3] multiplied by $(\alpha/\pi s^2)N_c\, x_t$. The term $\bar{f}^{(2)}_{add}(s^2)$ is given in Eq.(A1) of Ref. [4].

References

[1] D. Bardin et al., in "Reports of the Working Group on Precision Calculations for the Z-resonance", CERN Yellow Report, CERN 95-03, D. Bardin, W. Hollik, and G. Passarino eds, p. 7.

[2] G. Degrassi, S. Fanchiotti, F. Feruglio, P. Gambino, A. Vicini, *Phys. Lett.* **B350** (1995) 75 and "Reports of the Working Group on Precision Calculations for the Z-resonance", CERN Yellow Report, CERN 95-03, D. Bardin, W. Hollik, and G. Passarino eds, p. 163.

[3] G. Degrassi, P. Gambino, and A. Vicini, *Phys. Lett.* **B383** (1996) 219.

[4] G. Degrassi, P. Gambino, and A. Sirlin, *Phys. Lett.* **B394** (1997) 188.

[5] G. Degrassi, S. Fanchiotti, A. Sirlin, *Nucl. Phys.* **B351** (1991) 49.

[6] A. Sirlin, *Phys. Rev.* **D22** (1980) 971.

[7] G. Degrassi, P. Gambino, M. Passera, and A. Sirlin, *Phys. Lett.* **B418** (1998) 209.

[8] P. Gambino, talk presented at the IV Int. Symposium on Radiative Corrections (RADCOR 98), Barcelona, September 1998; to appear in the Proceedings, ed. J.Sola; hep-ph/9812332.

[9] G. Degrassi, *Acta Phys. Pol.* **B29** (1998) 2683.

[10] G. Degrassi and G. D'Agostini, hep-ph/9902226, to appear on *Eur. Phys. J.* **C**.

[11] K. Aoki, Z. Hioki, R. Kawabe, M. Konuma, and T. Muta, *Suppl. Progr. Theor. Phys.* **73** (1982) 1.

[12] M. Böhm, W. Hollik, and H. Spiesberger, *Fortschr. Phys.* **34** (1986) 687; P.A. Grassi, *Nucl. Phys.* **B537** (1999) 527.

[13] J.C. Taylor, *Gauge Theories of Weak Interactions*, Cambridge University Press, Cambridge, 1976.

[14] A. Sirlin and R. Zucchini, *Nucl. Phys.* **B266** (1986) 389.

[15] G. Ross and J.C. Taylor, *Nucl. Phys.* **B51** (1973) 125.

[5] Eq.(7b) of Ref. [3] has a misprint in the fourth term of the first line. The correct term is $77c^2/72$ instead of $77c^2/12$ as printed in Ref. [3]. We thank G. Passarino for pointing this out to us.

[16] A. Sirlin, *Phys. Lett.* **B232** (1989) 123.

[17] R. Stuart, *Phys. Lett.* **B262** (1991) 113; A. Sirlin, *Phys. Rev. Lett.* **67** (1991) 2127; M. Passera and A. Sirlin, *Phys. Rev.* **D58** (1998) 113010.

[18] P. Gambino, *Acta Phys. Pol.* **B27**, 3671 (1996).

[19] K. Fujikawa, *Phys. Rev.* **D7** (1973) 393.

[20] J.C. Romão and A. Barroso, *Phys. Rev.* **D35** (1987) 2836.

[21] F. Boudjema and E. Chopin, *Z. Phys.* **C73** (1996) 85.

[22] R. Scharf, Diploma Thesis, Würzburg, 1991; D.J. Broadhurst, *Z. Phys.* **C47** (1990) 115.

[23] S. Bauberger, M. Böhm, *Nucl. Phys.* **B445** (1995) 25; A. Czarnecki, U. Kilian, D. Kreimer, *Nucl. Phys.* **B433** (1995) 259; A. Ghinculov, J.J. van der Bij, *Nucl. Phys.* **B436** (1995) 30.

[24] R. Barbieri *et al.*, *Phys. Lett.* **B288** (1992) 95 and *Nucl. Phys.* **B409** (1993) 105; J. Fleischer, O.V. Tarasov, F. Jegerlehner, *Phys. Lett.* **B319** (1993) 249; G. Degrassi, S. Fanchiotti, and P. Gambino, *Int. J. Mod. Phys.* **A10**, (1995) 1337.

[25] A.T. Davydychev and B. Tausk, *Nucl. Phys.* **B397** (1993) 123; J. Fleischer and O.V. Tarasov, *Z. Phys.* **C64** (1994) 413.

[26] S.G. Gorishny, *Nucl. Phys.* **B319** (1989) 633; S.G. Gorishny and S.A. Larin, *Nucl. Phys.* **B283** (1987) 452; K.G. Chetyrkin, *Teor. Mat. Fiz.* **75** (1988) 26, and preprint MPI/PAE/PTh 13/81 (Munich 1991); F.V. Tkachov, *Int. J. Mod. Phys.* **A8** (1993) 2047; G.B. Pivovarov and F.V. Tkachov, *Int. J. Mod. Phys.* **A8** (1993) 2241; V.A. Smirnov, *Mod. Phys. Lett.* **A10**, (1995) 1485,

[27] F.A. Berends *et al.*, *Nucl. Phys.* **B439** (1995) 536; J. Fleischer, V.A. Smirnov, O.V. Tarasov, *Z. Phys.* **C74** (1997) 379.

[28] F.A. Berends, A.T. Davydychev, V.A. Smirnov, *Nucl. Phys.* **B478** (1996) 59.

[29] R. Harlander, T. Seidensticker, and M. Steinhauser, *Phys. Lett.* **B426** (1998) 125; P. Gambino, A. Kwiatkowski, N. Pott, *Nucl. Phys.* **B544** (1999) 532.

[30] S. Bauberger and G. Weiglein, *Phys. Lett.* **B419** (1998) 333; G. Weiglein, hep-ph/9901317.

[31] P. Gambino, A. Sirlin, and G. Weiglein, hep-ph/9903249, JHEP 9904 (1999) 025.

[32] G. Degrassi, A. Sirlin, *Nucl. Phys.* **B352** (1991) 342.

[33] P. Gambino and A. Sirlin, *Phys. Rev.* **D49** (1994) R1160.

[34] W. Marciano and A. Sirlin, *Phys. Rev.* **D22** (1980) 2695.

[35] M. Consoli, W. Hollik, F. Jegerlehner, *Phys. Lett.* **B227** (1989) 167.

[36] A. Djouadi, *Nuovo Cimento* **100A** (1988) 357; A. Djouadi and C. Verzegnassi, *Phys. Lett.* **B195** (1987) 265; B.A. Kniehl, *Nucl. Phys.* **B347** (1990) 86; A. Djouadi, P. Gambino, *Phys. Rev.* **D49** (1994) 3499, E: *ibid.* **D53** (1996) 4111.

[37] S. Fanchiotti, B.A. Kniehl, A. Sirlin, *Phys. Rev.* **D48** (1993) 307.

[38] K. Chetyrkin, J.H. Kühn, M. Steinhauser, *Phys. Lett.* **B351** (1995) 331, *Phys. Rev. Lett.* **75** (1995) 3394 and *Nucl. Phys.* **B482** (1996) 213 (and refs therein); L. Avdeev *et al.*, *Phys. Lett.* **B336** (1994) 560; **B349**, 597 (E) (1995).

[39] A. Sirlin, *Phys. Lett.* **B348** (1995) 201, and in *Reports of the Working Group on Precision Calculations for the Z resonance*, CERN 95-03.

[40] D. Bardin and G. Passarino, hep-ph/9803425; D. Bardin, M. Grunewald, and G. Passarino, hep-ph/9902452.

[41] R. Stuart and T. van Ridberger, *Phys. Rev. Lett.* **82** (1999) 488; see also A. Ferroglia, G. Ossola, A. Sirlin, hep-ph/9905442.

[42] The LEP and SLD Electroweak Working Groups, preprint CERN-EP/99-15, February 1999; for the most recent preliminary results, see `http://www.cern.ch/LEPEWWG`.

[43] S. Eidelman, F. Jegerlehner, *Z. Phys.* **C67** (1995) 585; H. Burkhardt, B. Pietrzyk, *Phys. Lett.* **B356** (1995) 398; M. Swartz, *Phys. Rev.* **D53** (1996) 5268.

[44] M. Davier and S. Hocker, *Phys. Lett.* **B435** (1998) 427; J.H. Kühn and M. Steinhauser, *Phys. Lett.* **B437** (1998) 425; S. Groote *et al.*, *Phys. Lett.* **B440** (1998) 375; J. Erler, *Phys. Rev.* **D59** (1999) 054008, F. Jegerlehner, hep-ph/9901386.

[45] D. Bardin *et al.*, `ZFITTER 4.9`, hep-ph/9412201; D. Bardin, in preparation.

[46] G. Montagna, O. Nicrosini, F. Piccinini, G. Passarino, hep-ph/9804211.

[47] J. Erler and P. Langacker, p. 90 of Particla Data Group: C. Caso *et al.*, *Eur. Phys. J.* **C3** (1998) 1; hep-ph/9809352.

[48] G. Degrassi and A. Sirlin, *Phys. Rev.* **D46** (1992) 3104.

[49] M. Machacek and M. Vaughn, *Nucl. Phys.* **B222** (1983) 83.

[50] A. Czarnecki and J.H Kühn, *Phys. Rev. Lett.* **77** (1996) 3955.